

# A Theoretical Study of Inductive Biases in Contrastive Learning

Jeff Z. HaoChen   Tengyu Ma

Stanford University  
Department of Computer Science

{jhaochen, tengyuma}@cs.stanford.edu

## Abstract

Understanding self-supervised learning is important but challenging. Previous theoretical works study the role of pretraining losses, and view neural networks as general black boxes. However, the recent work of [Saunshi et al. \(2022\)](#) argues that the model architecture — a component largely ignored by previous works — also has significant influences on the downstream performance of self-supervised learning. In this work, we provide the first theoretical analysis of self-supervised learning that incorporates the effect of inductive biases originating from the model class. In particular, we focus on contrastive learning — a popular self-supervised learning method that is widely used in the vision domain. We show that when the model has limited capacity, contrastive representations would recover certain special clustering structures that are compatible with the model architecture, but ignore many other clustering structures in the data distribution. As a result, our theory can capture the more realistic setting where contrastive representations have much lower dimensionality than the number of clusters in the data distribution. We instantiate our theory on several synthetic data distributions, and provide empirical evidence to support the theory.

## 1 Introduction

Recent years have witnessed the effectiveness of pre-trained representations, which are learned on unlabeled data with self-supervised losses and then adapted to a wide range of downstream tasks ([Brown et al., 2020](#), [Caron et al., 2020](#), [Chen et al., 2020b,c](#), [Chen and He, 2020](#), [Chen et al., 2020d](#), [Gao et al., 2021](#), [He et al., 2020](#), [Radford et al., 2019](#), [Su et al., 2021](#)). However, understanding the empirical success of this emergent pre-training paradigm is still challenging. It requires novel mathematical frameworks and analyses beyond the classical statistical learning theory. The prevalent use of deep neural networks in self-supervised learning also adds to the mystery.

Many theoretical works focus on isolating the roles of self-supervised losses, showing that they encourage the representations to capture certain structures of the unlabeled data that are helpful for downstream tasks ([Arora et al., 2019](#), [HaoChen et al., 2021, 2022](#), [Saunshi et al., 2020](#), [Wei et al., 2021](#), [Xie et al., 2021](#)). However, these works oftentimes operate in the sufficient pre-training data (polynomial in the dimensionality) or even infinite pre-training data regime, and view the neural network as a *black box*. The only relevant property of neural networks in these works is that they form a parameterized model class with finite complexity measure (e.g., Rademacher complexity).

Recently, [Saunshi et al. \(2022\)](#) argue that the pre-training loss is *not* the only contributor to the performance of self-supervised learning, and that previous works which view neural networks as a black box cannot tell apart the differences in downstream performance between architectures (e.g., ResNet ([He et al., 2015](#)) vs vision transformers ([Dosovitskiy et al., 2020](#))). Furthermore, self-supervised learning with an appropriate architecture can possibly work under more general condi-

tions and/or with fewer pre-training data than predicted by these results on general architecture. Therefore, a more comprehensive and realistic theory needs to take into consideration the inductive biases of architecture.

This paper provides the first theoretical analyses of the inductive biases of *nonlinear* architectures in self-supervised learning. Our theory follows the setup of the recent work by HaoChen et al. (2021) on contrastive learning and can be seen as a refinement of their results by further characterizing the model architecture’s impact on the learned representations.

We recall that HaoChen et al. (2021) show that contrastive learning, with sufficient data and a parameterized model class of finite complexity, is equivalent to spectral clustering on a so-called *population positive-pair graph*, where nodes are augmented images and an edge between the nodes  $x$  and  $x'$  is weighted according to the probability of encountering  $(x, x')$  as a positive pair. They essentially assume that the positive-pair graph contains several major semantically-meaningful clusters, and prove that contrastive representations exhibit a corresponding clustering structure in the Euclidean space, that is, images with relatively small graph distance have nearby representations.

Their results highly rely on the clustering property of the graph—the representation dimensionality and pre-training sample complexity both scale in the number of clusters. The important recent work of Saunshi et al. (2022), however, demonstrates with a synthetic setting that contrastive learning can provably work with linear model architectures even if the number of clusters is huge (e.g., exponential in the dimensionality). Beyond the simple synthetic example discussed in their paper, there has been no previous work that formally characterizes this effect in a general setting.

In this work, we develop a general theory that leverages the inductive bias to avoid the dependency on the potentially huge number of clusters: although there exists a large number of clusters in the positive-pair graph, the number of clusters *implementable by the model* (which we call *minimal implementable clusters*) could be much smaller, even exponentially. Figure 1 shows an example where a linear function can only implement one clustering structure but not the other, despite both being valid clusters in the positive-pair graph. It’s possible that a minimal implementable cluster consists of multiple well-separated sub-clusters but none of these sub-clusters can be implemented by the model class.

We show that contrastive representations would only recover the clustering structures that are compatible with the model class, hence low-dimensional contrastive learned representations would work well on the downstream tasks. Concretely, suppose the number of minimal implementable clusters is  $r$  which can be much smaller than the number of natural clusters in the graph  $r_0$ . HaoChen et al. (2021) prove the efficacy of contrastive learning assuming the representation dimensionality (hence also sample complexity) is larger than  $r_0$ . We develop a new theory (Theorem 3.6) that makes the representation dimensionality only depend on  $r$  instead of  $r_0$ . We also extend this result to a more complex setting where we can deal with even more structured clusters, e.g., when there are  $2^s$  clusters with certain geometric structures, but the representation dimensionality can scale with only  $s$  instead of  $2^s$ . See Theorem 4.4 and its instantiation on Example 5.1 for this result.

We instantiate our theory on several synthetic data distributions and show that contrastive learning with appropriate model architectures can reduce the representation dimensionality, allowing better sample complexity. We consider a data distribution on a hypercube first proposed by Saunshi et al. (2022) which contains a small subspace of features that are invariant to data augmentation and a large subspace of spurious features. When the function class is linear, we show that the contrastive representations can solve downstream binary classification tasks if the downstream label only depends on one dimension of invariant features (Theorem 5.3). When the function

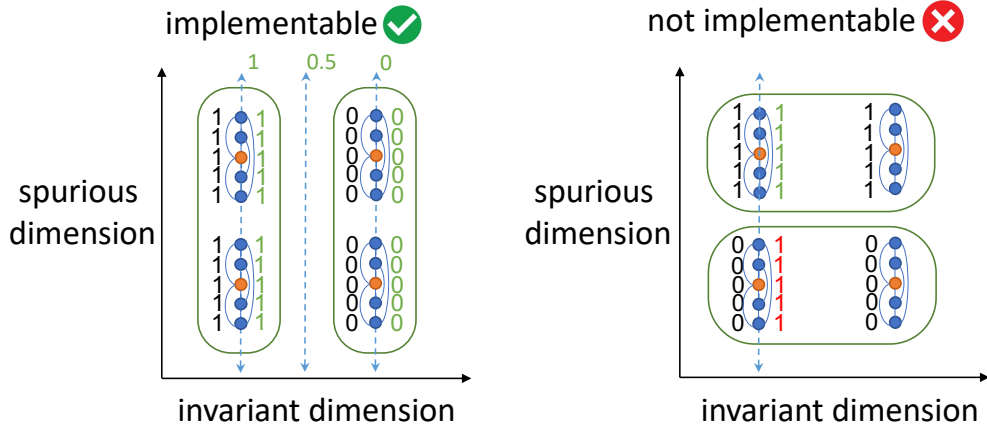


Figure 1: **A simple example where the linear function class learns the correct feature and ignores the spurious feature.** A simplified version of the synthetic example proposed in the work of Saunshi et al. (2022). The orange points are the original data and blue points are augmented data (obtained by adding noise in the spurious dimension). The dimension invariant to augmentation is desired. Edges represent positive pairs that are constructed from augmentation. We say a real-valued function *implements* a cluster if it outputs 1 on the cluster and outputs 0 on all other data. We note that here implementing means matching the *exact* value, rather than simply matching the label after applying some linear threshold. The figure above shows two possible ways to partition the data into two clusters, but only the one on the left-hand side (which captures the invariant dimension) is implementable by a linear function. Here we use black numbers to indicate the target output on the data, and green numbers to indicate the output of the implementing function which extrapolates outside of the data support. Note that linear model is *not* composed with a threshold function. The partition on the right hand side is not implementable because any linear model that outputs constant 1 on the upper-left small cluster would also output 1 on the bottom-left small cluster due to linear extrapolation. Here we use red numbers to indicate the output of the linear function that contradicts with the target.

class is ReLU networks (hence more expressive), we show that the contrastive representations can solve more diverse downstream classification problems where the label can depend on all invariant features (Theorem 5.6). We also provide examples for Lipschitz-continuous function classes (Theorem 5.9) and convolutional neural networks (Theorem 5.12).

We provide experimental results to support our theory. We propose a method to test the number of implementable clusters of ResNet-18 on the CIFAR-10 dataset and show that there are indeed only a small number of implementable clusters under the model architecture constraint (Section 6).

## 2 Related works

Contrastive learning learns representations from different views or augmentations of inputs (Bachman et al., 2019, Bardes et al., 2021, Caron et al., 2020, Chen et al., 2020a, Chen and He, 2021, Dubois et al., 2022, Gao et al., 2021, Henaff, 2020, Hjelm et al., 2018, Misra and Maaten, 2020, Oord et al., 2018, Robinson et al., 2021, Tian et al., 2019, 2020, Wu et al., 2018, Ye et al., 2019, Zbontar et al., 2021). The learned representation can be used (either directly or after finetuning) to solve a wide range of downstream tasks with high accuracy.

The empirical success of contrastive learning has attracted a series of theoretical works that study the contrastive loss (Arora et al., 2019, Ash et al., 2022, HaoChen et al., 2021, 2022, Lee et al., 2020, Nozawa and Sato, 2021, Tian, 2022, Tosh et al., 2020, 2021, Wang et al., 2021), most of which treat the model class as a black box except for the work of Lee et al. (2020) which studies the learned representation with linear models, and the works of Tian (2022) and Wen and Li (2021) which study the training dynamics of contrastive learning for linear and 2-layer ReLU networks. Most related to our work is Saunshi et al. (2022) which theoretically shows (on a linear toy example) that appropriate model classes help contrastive learning by reducing the sample complexity. We generalize their results to broader settings.

Several theoretical works also study non-contrastive methods for self-supervised representation learning (Balestriero and LeCun, 2022, Garrido et al., 2022, Tian et al., 2021, Wen and Li, 2022). Garrido et al. (2022) establish the duality between contrastive and non-contrastive methods. Balestriero and LeCun (2022) provide a unified framework for contrastive and non-contrastive methods. There are also works theoretically studying self-supervised learning in other domains such as language modeling (Saunshi et al., 2020, Wei et al., 2021, Xie et al., 2021).

### 3 From clusters to minimal implementable clusters

In this section, we introduce our main theoretical results regarding the role of inductive biases of architectures in contrastive learning. Recall that contrastive learning encourages two different views of the same input (also called a *positive pair*) to have similar representations, while two random views of two different inputs (also called a *negative pair*) have representations that are far from each other. Formally, we use  $p_{\text{data}}$  to denote the distribution of a random view of random input, use  $p_{\text{pos}}$  to denote the distribution of a random positive pair, and  $\mathcal{X}$  to denote the support of  $p_{\text{data}}$ . For instance,  $\mathcal{X}$  is the set of all augmentations of all images for visual representation learning.

Following the setup of HaoChen et al. (2022), for a representation map  $f : \mathcal{X} \rightarrow \mathbb{R}^k$  where  $k$  is the representation dimensionality, we learn the contrastive representation by minimizing the following generalized spectral contrastive loss:

$$\mathcal{L}_\lambda(f) := \mathbb{E}_{(x, x^+) \sim p_{\text{pos}}} [\|f(x) - f(x^+)\|_2^2] + \lambda \cdot R(f), \quad (1)$$

where  $\lambda > 0$  is a hyperparameter indicating the regularization strength, and the regularizer normalizes the representation covariance towards the identity matrix:

$$R(f) := \left\| \mathbb{E}_{x \sim p_{\text{data}}} [f(x)f(x)^\top] - \mathbb{I} \right\|_F^2. \quad (2)$$

This loss is very similar to the popular Barlow Twins loss (Zbontar et al., 2021) and has been shown to empirically work well (HaoChen et al., 2021). Theoretically, the prior work proposes the notion of *positive-pair graph* with  $\mathcal{X}$  being the vertex set and an edge between the nodes  $x$  and  $x'$  is weighted according to the probability of encountering  $(x, x')$  as a positive pair (i.e.,  $p_{\text{pos}}(x, x')$ ). This graph is defined on the **population** data, and intuitively captures the semantic relationship between different data — when the positive pairs are formed by applying data augmentation to the same natural data, it is expected that datapoints in the same cluster in the positive-pair graph would have similar semantic meanings. Figure 2 gives a demonstration of the positive-pair graph.

Their analysis shows that learning contrastive representations with the above loss is equivalent to spectral clustering (Ng et al., 2001, Shi and Malik, 2000) on this positive-pair graph, hence can learn meaningful representations when the graph has clustering structures.

Different from the prior work, we study the representation map that minimizes the contrastive loss *within a certain function class*  $\mathcal{F}$ . Here we assume functions in  $\mathcal{F}$  map data in  $\mathcal{X}$  to representa-

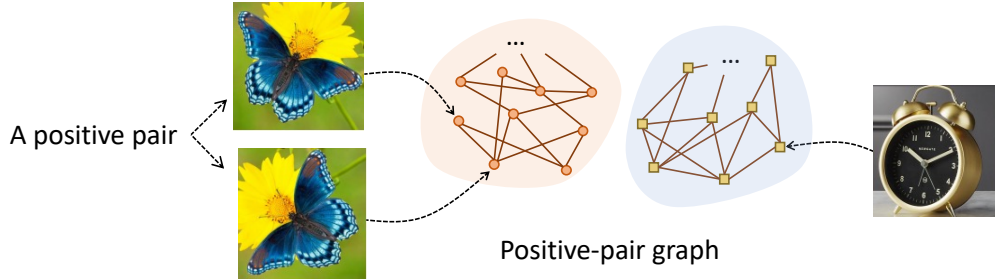


Figure 2: **A demonstration of the positive-pair graph.** When the positive pairs are formed by applying data augmentation (such as rotation) to the same natural image, data with the same semantic meaning (e.g., the two butterfly images) tend to belong to the same cluster in the positive-pair graph. Datapoints with different semantic meanings (e.g., a butterfly image and a clock image) would not be connected in the positive-pair graph, hence belong to different clusters.

tions in  $\mathbb{R}^k$  for some dimensionality  $k$ . The main contribution of our result is the improvement of  $k$  due to the consideration of this specific function class: by studying the representation learned within a constrained model class  $\mathcal{F}$ , we will show that the necessary representation dimensionality  $k$  is much smaller than that required in the prior work. As a result, the sample complexity for the downstream labeled task would be improved compared to the prior work.

Let  $\{S_1, S_2, \dots, S_m\}$  be a  $m$ -way partition of  $\mathcal{X}$ , i.e., they are disjoint non-empty subsets of  $\mathcal{X}$  such that  $\mathcal{X} = \cup_{i \in [m]} S_i$ . For any  $x \in \mathcal{X}$ , let  $\text{id}_x$  be the index such that  $x \in S_{\text{id}_x}$ . We consider a partition of the graph such that there is not much connection between any two clusters, which is formalized by the following assumption.

**Assumption 3.1** ( $\alpha$ -separability). *The probability of a positive pair belonging to two different sets is less than  $\alpha$ :*

$$\Pr_{(x, x^+) \sim p_{\text{pos}}} (\text{id}_x \neq \text{id}_{x^+}) \leq \alpha. \quad (3)$$

We consider downstream tasks that are  $r$ -way classification problems with label function  $y(\cdot) : \mathcal{X} \rightarrow [r]$ . We assume that the downstream task aligns with the clusters:

**Assumption 3.2.** *The downstream label  $y(x)$  is a constant on each  $S_i$ .*

Our key assumptions about the function class are that it can implement desirable clustering structures (Assumption 3.4) but cannot break the positive-pair graph into too many clusters (Assumption 3.3).

Let  $S \subset \mathcal{X}$  be a subset of  $\mathcal{X}$ ,  $p_{\text{data}}^S$  be the distribution  $p_{\text{data}}$  restricted to set  $S$ , and  $p_{\text{pos}}^S$  be the positive pair distribution  $p_{\text{pos}}$  conditioned on both datapoints in the pair belonging to set  $S$ . For any function  $g : S \rightarrow \mathbb{R}$ , we define the following expansion quantity:

$$Q_S(g) := \frac{\mathbb{E}_{(x, x^+) \sim p_{\text{pos}}^S} [(g(x) - g(x^+))^2]}{\mathbb{E}_{x \sim p_{\text{data}}^S, x' \sim p_{\text{data}}^S} [(g(x) - g(x'))^2]}. \quad (4)$$

We let  $Q_S(g) = \infty$  if the denominator is 0. Here the numerator represents the discrepancy between a random positive pair, and the denominator represents the global variance of  $g$ . Intuitively, a smaller value  $Q_S(g)$  means that function  $g$  does a better job at separating the set  $S$  into disjoint sub-clusters, and hence implements an inner-cluster connection structure that is sparse. For instance,

if  $S$  contains two disjoint sub-clusters, and  $g$  has different constant values on each of them, then  $Q_S(g) = 0$ . On the other hand, if  $S$  is densely connected, then  $Q_S(g) > 0$  regardless of the choice of  $g$ . We also note that  $Q_S(\cdot)$  is also closely related to the sparsest cut formulation in spectral graph theory. When  $g$  is restricted to output only values in  $\{0, 1\}$ , then the RHS of equation 4 is the sparsest cut value of the subgraph supported on the vertices in  $S$  (cf. Definition 4 or equation 2.3 of Trevisan (2015)), and  $Q_S$  is also a typical way to relax the sparsest cut value (cf. Section 2.3 of Trevisan (2015)).

The first assumption about the function class  $\mathcal{F}$  assumes that no function in the class can break one cluster into two well-separated sub-clusters:

**Assumption 3.3** ( $\mathcal{F}$ -implementable inner-cluster connection larger than  $\beta$ ). For any function  $f \in \mathcal{F}$  and any linear head  $w \in \mathbb{R}^k$ , let function  $g(x) = w^\top f(x)$ . For any  $i \in [m]$  we have that:

$$Q_{S_i}(g) \geq \beta. \quad (5)$$

We note that when the function class  $\mathcal{F}$  contains *all* the functions from  $\mathcal{X}$  to  $\mathbb{R}^k$ , Assumption 3.3 essentially says that each of  $\{S_1, S_2, \dots, S_m\}$  has large internal expansion, hence recovers Assumption 3.5 in HaoChen et al. (2021). However, when  $\mathcal{F}$  has limited capacity, each cluster  $S_i$  can still contain well-separated sub-clusters, but just those sub-clusters cannot be implemented by functions in  $\mathcal{F}$ .

Assumption 3.3 implies that the function class cannot be too expressive. However, in order for the learned representation map to be useful for downstream tasks, it needs to be expressive enough to represent the useful information. Thus, we introduce the following assumption on the function class.

**Assumption 3.4** (Implementability). Recall that  $\text{id}_x$  is the index such that  $x \in S_{\text{id}_x}$ . There exists a function  $f \in \mathcal{F}$  such that  $f(x) = e_{\text{id}_x}$  for all  $x \in p_{\text{data}}$  where  $e_i \in \mathbb{R}^m$  is the vector where the  $i$ -th dimension is 1 and other dimensions are 0.

When both Assumption 3.3 and Assumption 3.4 hold, we say  $\{S_1, S_2, \dots, S_m\}$  are *minimal implementable clusters* with respect to  $\mathcal{F}$ .

We also introduce the following Assumption 3.5 which is true for any function class implemented by a neural network where the last layer is linear. We note that this assumption is needed only for the technical rigour of the proof, and is not essential to the conceptual message of our theory.

**Assumption 3.5** (Closure under scaling). For any function  $f \in \mathcal{F}$  and vector  $u \in \mathbb{R}^m$ , define function  $f'(x) = u \odot f(x)$  where  $\odot$  means element-wise product. Then, we have  $f' \in \mathcal{F}$ .

Let  $P_{\min} := \min_{i \in [m]} \Pr_{x \sim p_{\text{data}}}(x \in S_i)$  and  $P_{\max} := \max_{i \in [m]} \Pr_{x \sim p_{\text{data}}}(x \in S_i)$  be the sizes of the smallest and largest sets respectively. Under the above assumptions, we have the following theorem that shows learning a representation map within  $\mathcal{F}$  and representation dimensionality  $k = m$  can solve the downstream task:

**Theorem 3.6.** Suppose  $\{S_1, S_2, \dots, S_m\}$  are minimal implementable clusters with respect to  $\mathcal{F}$  (i.e., Assumptions 3.1 and 3.3 hold), and the function class  $\mathcal{F}$  satisfies Assumptions 3.4 and 3.5. For  $\lambda > \alpha/P_{\min}$ , consider a learned representation map  $\hat{f} = \arg \min_{f \in \mathcal{F}} \mathcal{L}_\lambda(f)$  that minimizes the contrastive loss. Then, when  $k = m$ , for any downstream task that satisfies Assumption 3.2, there exists a linear head  $W \in \mathbb{R}^{r \times k}$  which achieves downstream error

$$\mathbb{E}_{x \sim p_{\text{data}}} [\|W \hat{f}(x) - e_{y(x)}\|_2^2] \leq \frac{\alpha}{\beta} \cdot \frac{P_{\max}}{P_{\min} - \alpha}. \quad (6)$$

We note that  $P_{\max} \approx P_{\min}$  when the partitions are balanced. Thus, so long as  $\alpha \ll P_{\min}$  (i.e., the probability of a positive pair crossing different clusters is smaller than the probability of it containing data from the smallest cluster), the right-hand side is roughly  $\alpha/\beta$ . Thus, when the inter-cluster connection  $\alpha$  is smaller than the inner-cluster connection that is implementable by the function class  $\beta$ , the downstream accuracy would be high.

**Comparison with HaoChen et al. (2021).** We note that our result requires  $k = m$ , whereas HaoChen et al. (2021) provide analysis in a more general setting for arbitrary  $k$  that is large enough. Thus, when the function class  $\mathcal{F}$  is the set of all functions, our theorem recovers a special case of HaoChen et al. (2021). Our result requires a stricter choice of  $k$  mainly because when  $\mathcal{F}$  has limited capacity, a higher dimensional feature may contain a lot of “wrong features” while omitting the “right features”, which we discuss in more details in the next section.

## 4 An eigenfunction viewpoint

In this section, we introduce an eigenfunction perspective that generalizes the theory in the previous section to more general settings. We first introduce the background on eigenfunctions and discuss its relation with contrastive learning. Then we develop a theory that incorporates the model architecture with assumptions stated using the language of eigenfunctions. The advantage over the previous section is that we can further reduce the required representation dimensionality when the minimal implementable clusters exhibit certain internal structures.

Here we note that we use the language of eigenfunctions because the positive-pair graph can be infinite. Causal readers can think of the the graph as a very large but finite graph and treat all the eigenfunctions as eigenvectors.

Our theory relies on the notion of *Laplacian operator*  $\mathbb{L}$  of the positive-pair graph, which maps a function  $g : \mathcal{X} \rightarrow \mathbb{R}$  to another function  $\mathbb{L}(g) : \mathcal{X} \rightarrow \mathbb{R}$  defined as follows.

$$\mathbb{L}(g)(x) := g(x) - \int \frac{p_{\text{pos}}(x, x')}{p_{\text{data}}(x)} g(x') dx'. \quad (7)$$

We say a function  $g$  is an eigenfunction of  $\mathbb{L}$  with eigenvalue  $\psi \in \mathbb{R}$  if for some scalar  $\psi$

$$\mathbb{E}_{x \sim p_{\text{data}}} [(\psi \cdot g(x) - \mathbb{L}(g)(x))^2] = 0. \quad (8)$$

This essentially means that  $L(g) = \psi \cdot g$  on the support of  $p_{\text{data}}$ .

**Eigenfunctions with small eigenvalues achieve small loss on the positive-pairs.** One important property is that when  $g$  is an eigenfunction with small eigenvalue  $\psi$ , the quadratic form  $\mathbb{E}_{(x, x^+) \sim p_{\text{pos}}} [(g(x) - g(x^+))^2]$  is also small, that is, there is a good match between the positive-pairs. In particular, when  $\psi = 0$ , we have that  $\mathbb{L}(g)(x) = 0$  on the support of  $p_{\text{data}}$ . Thus,

$$\mathbb{E}_{(x, x^+) \sim p_{\text{pos}}} [(g(x) - g(x^+))^2] = 2\mathbb{E}_{x \sim p_{\text{data}}} [g(x)^2] - 2\mathbb{E}_{(x, x^+) \sim p_{\text{pos}}} [g(x)g(x^+)] \quad (9)$$

$$= 2\mathbb{E}_{x \sim p_{\text{data}}} [g(x)^2] - 2\mathbb{E}_{x \sim p_{\text{data}}} \left[ g(x) \int \frac{p_{\text{pos}}(x, x')}{p_{\text{data}}(x)} g(x') dx' \right] \quad (10)$$

$$= 2\mathbb{E}_{x \sim p_{\text{data}}} [g(x)^2] - 2\mathbb{E}_{x \sim p_{\text{data}}} [g(x)^2] = 0. \quad (11)$$

We can formalize this property of eigenfunctions with the following proposition.

**Proposition 4.1.** *Any function  $g : \mathcal{X} \rightarrow \mathbb{R}$  that satisfies  $\mathbb{E}_{(x, x^+) \sim p_{\text{pos}}} [(g(x) - g(x^+))^2] = 0$  is an eigenfunction of  $\mathbb{L}$  with eigenvalue 0.*

**Clusters can be represented by small eigenfunctions.** Intuitively, small eigenfunctions (i.e., eigenfunctions with small eigenvalues) correspond to disconnected clusters in the positive-pair graph.

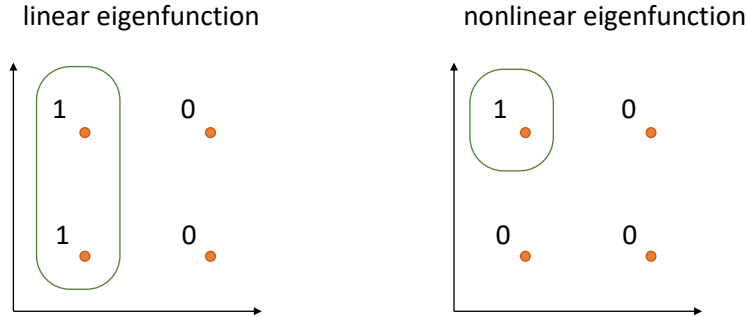


Figure 3: **Eigenfunctions capture the geometric relationship between clusters.** Consider four disconnected clusters / nodes in the 2-dimensional Euclidean space. Since each cluster gives an eigenfunction, there is a subspace of 4 eigenfunctions that describes all the possible partitions. However, two of them are special—the two eigenfunctions that group the four clusters into two groups of two clusters along the axis—in the sense that they are linear. Therefore, the eigenfunction viewpoint helps us distinguish these special groupings from the others: when constrained to be linear, an eigenfunction can represent the clustering in the left figure but not that in the right figure. We note that the cluster in the left figure is not a minimal implementable cluster under our current definition in Section 3, since there exists a linear function within the function class that can separate it into two halves with zero connection.

To see this, let  $S$  be a cluster that is disconnected from the rest of the positive-pair graph. Let  $g$  implement the indicator function of  $S$ , i.e.,  $g(x) = 1$  if  $x \in S$ , and  $g(x) = 0$  if  $x \notin S$ . Since  $S$  is disconnected from the rest of the graph,  $p_{\text{pos}}(x, x')$  is non-zero only if  $x$  and  $x'$  both belong to  $S$  or both are not in  $S$ . As a result, one can verify that  $\mathbb{L}(g)(x) = 0$  for all  $x$ , thus  $g$  is an eigenfunction with eigenvalue 0. More generally, eigenfunctions with small but non-zero eigenvalues would correspond to clusters that are almost disconnected from the rest of the graph. This correspondance is well-known in the spectral graph theory literature (Trevisan, 2017).

**Eigenfunctions can capture more information than clustering.** Although clusters correspond to eigenfunctions with small eigenvalues, eigenfunctions could be more coarse-grained than clusters—e.g., one eigenfunction could represent two clusters because the sum of indicator functions of two disconnected clusters is also an eigenfunction. Therefore, when the clusters have some geometric structures with each other, the eigenfunctions could possibly help capture it. For instance, consider the situation where there are 4 disconnected clusters centered at a 2 by 2 grid, e.g.,  $\{0, 1\}^2$ . Since each cluster gives an eigenfunction, there is a subspace of 4 eigenfunctions. However, two of them are special—the two eigenfunctions that group the four clusters into two groups of two clusters along the axis—in the sense that they are linear, and therefore if the model family is restricted to be linear models, the linear inductive bias will prefer these two eigenfunctions over others. Figure 3 gives a demonstration of this example. We note that the cluster in the left figure of Figure 3 is not a minimal implementable cluster under our current definition in Section 3, since there exists a linear function within the function class that can separate it into two halves with zero connection. The eigenfunction viewpoint allows us to discuss these kind of structures.

In this section, we provide a generalized theory based on characterizing the implementability of eigenfunctions. Intuitively, we will assume that there exists  $k$  (and only  $k$ ) orthogonal eigenfunctions in the function class with very small eigenvalue, and the downstream task can be solved by these eigenfunctions. More precisely, let  $\phi \geq 0$  be a very small real number (which can be thought as



0 for casual readers). We assume  $\{f_{\text{eig}_i} : \mathcal{X} \rightarrow \mathbb{R}\}$  where  $i \in [m]$  are  $m$  approximate eigenfunctions with small eigenvalues, in the sense that

$$\sum_{i=1}^m \mathbb{E}_{(x,x^+) \sim p_{\text{pos}}} [\|f_{\text{eig}_i}(x) - f_{\text{eig}_i}(x^+)\|_2^2] \leq \phi. \quad (12)$$

We assume that they have unit norms:  $\forall i \in [m]$  we have

$$\mathbb{E}_{x \sim p_{\text{data}}} [f_{\text{eig}_i}(x)^2] = 1. \quad (13)$$

We also assume that they are orthogonal to each other in the sense that for any  $i \neq j$ ,

$$\mathbb{E}_{x \sim p_{\text{data}}} [f_{\text{eig}_i}(x) f_{\text{eig}_j}(x)] = 0. \quad (14)$$

Let  $f_{\text{eig}}(x) = [f_{\text{eig}_1}(x), f_{\text{eig}_2}(x), \dots, f_{\text{eig}_m}(x)]^\top$  be the vector-output representation map that concatenates the above  $m$  functions. We can write equation 12, equation 13, and equation 14 as

$$\mathbb{E}_{(x,x^+) \sim p_{\text{pos}}} [\|f_{\text{eig}}(x) - f_{\text{eig}}(x^+)\|_2^2] \leq \phi \quad (15)$$

and

$$\mathbb{E}_{x \sim p_{\text{data}}} [f_{\text{eig}}(x) f_{\text{eig}}(x)^\top] = \mathbb{I}. \quad (16)$$

Recall that our assumptions in the previous section intuitively say that even though a larger number of clusters exist in the positive-pair graph, many of them are not implementable by the function class. From the eigenfunction viewpoint, this means that only a small number of eigenfunctions with small eigenvalue are in the function class. Thus, we can make the following corresponding assumption which says that the vector-valued function  $f_{\text{eig}}$  contains all the implementable eigenfunctions with small eigenvalue.

**Assumption 4.2.** *Suppose a real-valued function  $g$  is implementable by  $\mathcal{F}$  (in the sense that  $g(x) = f(x)_i$  for some  $f \in \mathcal{F}$  and  $i \in [k]$ ) and is also an approximate eigenfunction with small eigenvalue in the sense that*

$$\mathbb{E}_{(x,x^+) \sim p_{\text{pos}}} [(g(x) - g(x^+))^2] \leq \tilde{\phi} \cdot \mathbb{E}_{x \sim p_{\text{data}}} [g(x)^2], \quad (17)$$

*then  $g$  must be a linear combination of  $f_{\text{eig}}$ , that is, there exists  $\tilde{w} \in \mathbb{R}^m$  such that*

$$\mathbb{E}_{x \sim p_{\text{data}}} [(\tilde{w}^\top f_{\text{eig}}(x) - g(x))^2] \leq \epsilon. \quad (18)$$

*Here both  $\tilde{\phi}$  and  $\epsilon$  are very small and can be thought as 0.*

We consider downstream tasks that can be solved by  $f_{\text{eig}}$ . Let  $\vec{y}(x) \in \mathbb{R}^r$  be a vector that represents the downstream label of data  $x$  (e.g., the one-hot embedding of the label when the downstream task is classification). We have the following assumption on the downstream task:

**Assumption 4.3.** *There exists a linear head  $W^* \in \mathbb{R}^{r \times m}$  with norm  $\|W^*\|_F \leq B$  such that*

$$\mathbb{E}_{x \sim p_{\text{data}}} [\|W^* f_{\text{eig}}(x) - \vec{y}(x)\|_2^2] \leq \zeta. \quad (19)$$

*Here  $\zeta$  can be thought of as a very small number.*

We have the following theorem using the above two assumptions:

**Theorem 4.4.** *Suppose function  $f_{\text{eig}} \in \mathcal{F}$  satisfies Assumptions 4.2 with  $(\tilde{\phi}, \epsilon)$  and Assumption 4.3 with  $(B, \zeta)$ . Suppose  $\tilde{\phi} > \phi$  or  $\tilde{\phi} = \phi = 0$ . Then, when  $k = m$ , for any  $\lambda > 0$  such that  $\phi \leq \tilde{\phi}(1 - \sqrt{\phi/\lambda})$  and learned representation map  $\hat{f} = \arg \min_{f \in \mathcal{F}} \mathcal{L}_\lambda(f)$ , there exists a linear head  $W \in \mathbb{R}^{r \times k}$  such that*

$$\mathbb{E}_{x \sim p_{\text{data}}} [\|W \hat{f}(x) - \vec{y}(x)\|_2^2] \lesssim \zeta + B^2 k (\epsilon + \frac{\phi}{\lambda}). \quad (20)$$

Since  $\zeta$ ,  $\epsilon$  and  $\phi$  are all very small values, the RHS of equation 20 is very small, hence the learned representation achieves small downstream error. As we will see in the first example in the next section, Theorem 4.4 indeed allows the representation dimensionality to be smaller than the number of minimal implementable clusters in the graph, hence generalizes the result in the previous section. The proof of Theorem 4.4 can be found in Section C.

**Relationship between Theorem 4.4 and Theorem 3.6.** In the setting of Theorem 3.6, the identity function of each minimal implementable cluster would be an achievable eigenfunction. Theorem 4.4 considers a more general situation than Theorem 3.6 where the minimal implementable clusters may not be well-defined, yet still we can show good results when the dimensionality  $k$  is equal to the number of achievable eigenfunctions  $m$ . We will mainly use Theorem 4.4 for the examples because it's more general and easier to be used, whereas we present Theorem 3.6 because it's more intuitive to understand. For instance, in our Example 5.1, Theorem 3.6 only applies when  $s = 1$ , whereas Theorem 4.4 applies for arbitrary  $s$ .

## 4.1 An end-to-end result

In this subsection, we provide an end-to-end result where both the representation function and the downstream linear head are learned from the empirical dataset. Given an empirical unlabeled pre-training dataset that contains  $n_{\text{pre}}$  positive pairs  $\{(x_1, x_1^+), (x_2, x_2^+), \dots, (x_{n_{\text{pre}}}, x_{n_{\text{pre}}}^+)\}$ , we define the empirical contrastive loss:

$$\widehat{\mathcal{L}}_\lambda(f) := \frac{1}{n_{\text{pre}}} \sum_{i=1}^{n_{\text{pre}}} \left( \|f(x_i) - f(x_i^+)\|_2^2 \right) + \lambda \cdot \left\| \sum_{i=1}^{n_{\text{pre}}} [f(x_i) f(x_i)^\top] - \mathbb{I} \right\|_F^2. \quad (21)$$

We introduce the following notion of Rademacher complexity of the function class  $\mathcal{F}$ .

**Definition 4.5** (Rademacher complexity). *We define the Rademacher complexity as*

$$\widehat{\mathcal{R}}_n(\mathcal{F}) = \mathbb{E}_{\substack{x_1 \sim p_{\text{data}}, \dots, x_n \sim p_{\text{data}} \\ \epsilon \sim \{-1, 1\}^n}} \left[ \sup_{f \in \mathcal{F}} \sup_{i \in [k]} \left| \frac{1}{n} \sum_{j=1}^n \epsilon_j f(x_j)_i \right| \right]. \quad (22)$$

We have the following theorem which gives an error bound when both the contrastive representation and the downstream linear head are learned from finite samples.

**Theorem 4.6.** *Let  $C_f$  be the upper bound of the feature norm, i.e.,  $\|f(x)\|_2 \leq C_f$  for all  $f \in \mathcal{F}$  and  $x \in \mathcal{X}$ . Suppose function  $f_{\text{eig}} \in \mathcal{F}$  satisfies Assumptions 4.2 with  $(\tilde{\phi}, \epsilon)$  and Assumption 4.3 with  $(B, \zeta)$ . Suppose  $\tilde{\phi} > 2\phi$ . Set  $k = m$  and  $\lambda \geq 2\tilde{\phi} + 1$ . Given a random sample of  $n_{\text{pre}}$  positive pairs from the pretraining distribution, we learn a representation map  $\hat{f} = \arg \min_{f \in \mathcal{F}} \widehat{\mathcal{L}}_\lambda(f)$ . Then, given  $n_{\text{ds}}$  labeled data from the downstream task  $\{(x_1, \tilde{y}(x_1)), (x_2, \tilde{y}(x_2)), \dots, (x_{n_{\text{ds}}}, \tilde{y}(x_{n_{\text{ds}}}))\}$ , we learn a linear head  $\widehat{W} \in \mathbb{R}^{r \times k}$  such that*

$$\widehat{W} := \arg \min_{W \text{ s.t. } \|W\|_F \leq 4B} \frac{1}{n_{\text{ds}}} \sum_{i=1}^{n_{\text{ds}}} \|W \hat{f}(x_i) - \tilde{y}(x_i)\|_2^2. \quad (23)$$

Then, with probability at least  $1 - \delta$ , we have

$$\begin{aligned} \mathbb{E}_{x \sim p_{\text{data}}} [\|\widehat{W} \hat{f}(x) - \tilde{y}(x)\|_2^2] &\lesssim \zeta + B^2 k \left( \epsilon + \frac{\phi}{\lambda} \right) \\ &+ \frac{C_f^4 k^2 \lambda + B^2 k}{\tilde{\phi} - 2\phi} \left( \widehat{\mathcal{R}}_{n_{\text{pre}}}(\mathcal{F}) + \sqrt{\frac{\log(k^2/\delta)}{n_{\text{pre}}}} \right) + BC_f \sqrt{\frac{\log(1/\delta)}{n_{\text{ds}}}}. \end{aligned} \quad (24)$$

We note that the unsupervised sample complexity depends on the Rademacher complexity of the function class, whereas the supervised sample complexity doesn't. The term  $BC_f$  intuitively captures the complexity of the learned representation, and usually increases as the feature dimensionality increases. The fact that the downstream sample complexity scales with  $BC_f$  demonstrates the benefit of learning a lower dimensional feature leveraging the inductive bias of the function class. The proof of Theorem 4.6 is in Section C.1.

## 5 Instantiations on several synthetic data distributions

In this section, we instantiate our previous theory on several examples of data distributions and show that when the model class has limited capacity, one can learn low-dimensional representations using contrastive learning and solve the downstream task with simple linear probing. In all of these examples, if we use a much more expressive model class, the representation dimensionality needs to be much higher, and hence more downstream samples are needed. These results demonstrate the benefit of leveraging inductive biases of the model architecture in contrastive learning.

### 5.1 Linear functions

Our first example is the hypercube example proposed in the work of Saunshi et al. (2022).

**Example 5.1.** *The natural data  $\bar{x} \sim \{-1, 1\}^d$  is the uniform distribution over the  $d$ -dimensional cube. Given a natural data  $\bar{x}$ , an augmented data  $x \sim \mathcal{A}(\bar{x})$  is sampled as follows: first uniformly sample  $d - s$  independent scalars  $\tau_{s+1} \sim [\frac{1}{2}, 1], \dots, \tau_d \sim [\frac{1}{2}, 1]$ , then scale the  $(s + 1)$ -th to  $d$ -th dimensions of  $\bar{x}$  with  $\tau_{s+1}, \dots, \tau_d$  respectively, while keeping the first  $s$  dimensions the same. Intuitively, the last  $d - s$  dimensions correspond to spurious features that can be changed by data augmentation, and the first  $s$  dimensions are invariance features that contain information about the downstream task. The downstream task is a binary classification problem, where the label  $y(x) = \text{sgn}(x_i)$  is the sign function of one of the first  $s$  dimensions  $i \in [s]$ .*

We consider contrastive learning with the linear function class defined below:

**Definition 5.2** (Linear function class). *Let  $U \in \mathbb{R}^{k \times d}$  be a matrix and we use  $f_U(x) = Ux$  to denote the linear function with weight matrix  $U$ . We define the  $k$ -dimensional linear function class as  $\mathcal{F}_{\text{linear}} = \{f_U : U \in \mathbb{R}^{k \times d}\}$ .*

Saunshi et al. (2022) directly compute the learned representations from contrastive learning. We can instantiate Theorem 4.4 to this example and get the following guarantees:

**Theorem 5.3.** *In Example 5.1, suppose we set the output dimensionality as  $k = s$  and learn a linear representation map that minimizes the contrastive loss  $\hat{f} = \arg \min_{f \in \mathcal{F}_{\text{linear}}} \mathcal{L}_\lambda(f)$  for any  $\lambda > 0$ . Then, there exists a linear head  $w \in \mathbb{R}^k$  with zero downstream error, that is,*

$$\mathbb{E}_{x \sim p_{\text{data}}} [(w^\top \hat{f}(x) - y(x))^2] = 0. \quad (25)$$

*In contrast, suppose the function class is the set of universal function approximators  $\mathcal{F}_{\text{uni}}$ . So long as the output dimensionality is no more than  $2^{d-1}$ , there exists solution  $\hat{f}' \in \arg \min_{f \in \mathcal{F}_{\text{uni}}} \mathcal{L}_\lambda(f)$  such that any linear head  $w \in \mathbb{R}^k$  has bad test error, that is*

$$\mathbb{E}_{x \sim p_{\text{data}}} [(w^\top \hat{f}'(x) - y(x))^2] \geq 1. \quad (26)$$

The proof of Theorem 5.3 is in Section D.1.

We note that as an implication of the lower bound, previous works that analyze universal function approximators (Arora et al., 2019, HaoChen et al., 2021, Tosh et al., 2021) wouldn't be able to show good downstream accuracy unless the representation dimensionality is larger than  $2^{d-1}$ . In contrast, our theory that incorporates the inductive biases of the function class manages to show that a much lower representation dimensionality  $k = s$  suffices.

We also note that this example shows a situation where Theorem 4.4 works but Theorem 3.6 doesn't, hence demonstrating how our theory derived from the eigenfunction viewpoint allows for lower representation dimensionality. There are  $2^s$  model-restricted minimal clusters in the graph, each encoded by one configuration of the  $s$  feature dimensions. Thus, applying Theorem 3.6 gives  $k = 2^s$  (which is worse than  $k = s$  but better than  $k = 2^d$ ). However, all the functions in  $\mathcal{F}_{\text{linear}}$  that implement some clusters span a  $s$ -dimensional subspace, thus we can find  $s$  eigenfunctions that satisfy Assumption 4.2. As a result, learning  $s$ -dimensional representations already suffices for solving the downstream task.

## 5.2 ReLU networks

In the previous example, the downstream task is only binary classification where the label is defined by one invariant feature dimension. Here we show that when we use a ReLU network as the model architecture, the linear probing can solve more diverse downstream tasks where the label can depend on the invariant feature dimensions arbitrarily.

**Example 5.4.** *The natural data distribution and the data augmentation are defined in the same way as Example 5.1. The downstream task is a  $m$ -way classification problem such that the label function  $y(\cdot) : \mathcal{X} \rightarrow [m]$  satisfies  $y(x) = y(x')$  if  $x_{1:s} = x'_{1:s}$ . In other words, the label only depends on the first  $s$  dimensions of the data.*

**Definition 5.5** (ReLU networks). *Let  $U \in \mathbb{R}^{k \times d}$  and  $b \in \mathbb{R}^k$ , we use  $f_{U,b} = \sigma(Wx + b)$  to denote the ReLU network with weight  $U$  and bias  $b$ , where  $\sigma$  is the element-wise ReLU activation. We define the  $k$ -dimensional ReLU network function class as  $\mathcal{F}_{\text{ReLU}} = \{f_{U,b} : U \in \mathbb{R}^{k \times d}, b \in \mathbb{R}^k\}$ .*

We have the following theorem which shows the effectiveness of the ReLU network architecture.

**Theorem 5.6.** *In Example 5.4, suppose we set the output dimensionality  $k = 2^s$  and learn a ReLU network representation map  $\hat{f} = \arg \min_{f \in \mathcal{F}_{\text{ReLU}}} \mathcal{L}_\lambda(f)$  for some  $\lambda > 0$ . Then, we can find a linear head  $W \in \mathbb{R}^{r \times k}$  with zero downstream error, that is,*

$$\mathbb{E}_{x \sim p_{\text{data}}} [\|W \hat{f}(x) - e_{y(x)}\|_2^2] = 0. \quad (27)$$

*In contrast, suppose the function class is the set of universal function approximators  $\mathcal{F}_{\text{uni}}$ . So long as the output dimensionality is no more than  $2^{d-s}$ , there exists solution  $\hat{f}' \in \arg \min_{f \in \mathcal{F}_{\text{uni}}} \mathcal{L}_\lambda(f)$  such that any linear head  $W \in \mathbb{R}^{m \times k}$  has bad test error, that is,*

$$\mathbb{E}_{x \sim p_{\text{data}}} [\|W \hat{f}'(x) - e_{y(x)}\|_2^2] \geq \frac{1}{2}. \quad (28)$$

When  $d \gg s$ , the above theorem shows that constraining the feature map to the ReLU networks can achieve good downstream performance with much smaller feature dimensionality. The proof of Theorem 5.6 is in Section D.2.

### 5.3 Lipschitz continuous functions

In many real-world settings where a neural network is trained with weight decay regularization and stochastic gradient descent, the resulting model usually has a limited weight norm and a relatively small Lipschitz constant (Jiang et al., 2019) partly because stochastic gradient descent implicitly prefers Lipschitz models, which tend to generalize better (Damian et al., 2021, Foret et al., 2020, Li et al., 2021, Wei and Ma, 2019, 2020). Here we provide an example showing that restricting the model class to Lipschitz continuous functions allows us to use lower dimensional representations. In particular, we consider the following example where a large number of clusters are located close to each other despite being disconnected in the positive-pair graph. Our result shows that contrastive learning with Lipschitz continuous functions would group those clusters together, allowing for lower representation dimensionality.

**Example 5.7.** Let  $S_1, S_2, \dots, S_r \subset \mathbb{R}^d$  be  $r$  manifolds in  $\mathbb{R}^d$ , each of which contains lots of disconnected subsets. Suppose the diameter of every manifold is no larger than  $\rho$ , that is for any  $i \in [r]$  and two data  $x, x' \in S_i$ , we have  $\|x - x'\|_2 \leq \rho$ . We also assume that different manifolds are separated by  $\gamma$ , that is for any  $i, j \in [r]$  such that  $i \neq j$ , and  $x \in S_i, x' \in S_j$ , we have  $\|x - x'\|_2 \geq \gamma$ . The data distribution  $p_{\text{data}}$  is supported on  $S_1 \cup S_2 \cup \dots \cup S_r$  and satisfies  $\Pr_{x \sim p_{\text{data}}}(x \in S_i) = 1/r$  for every  $i \in [r]$ . A positive pair only contains data from the same  $S_i$  (but not all pairs of datapoints from the same set need to be positive pairs). The downstream task is a  $m$ -way classification problem such that the label function  $y(\cdot) : \mathcal{X} \rightarrow [m]$  satisfies  $y(x) = y(x')$  if  $x$  and  $x'$  belong to the same set  $S_i$ .

We introduce the following family of Lipschitz continuous functions with parameter  $\kappa$ :

**Definition 5.8** ( $\kappa$ -Lipschitz continuous functions). A function  $f : \mathbb{R}^d \rightarrow \mathbb{R}^k$  is  $\kappa$ -Lipschitz if  $\|f(x) - f(x')\|_2 \leq \kappa \|x - x'\|_2$  for all  $x, x' \in \mathbb{R}^d$ . We define the  $\kappa$ -Lipschitz function class  $\mathcal{F}_{\text{Lip}, \kappa}$  as the set of all  $\kappa$ -Lipschitz continuous functions in  $\mathbb{R}^d \rightarrow \mathbb{R}^k$ .

We have the following theorem:

**Theorem 5.9.** In Example 5.7, suppose  $\kappa \geq \sqrt{2r}/\gamma$ . Let the output dimensionality  $k = r$  and learn a  $\kappa$ -Lipschitz continuous function  $\hat{f} \in \arg \min_{\mathcal{F}_{\text{Lip}, \kappa}} \mathcal{L}_\lambda(f)$  for some  $\lambda > 0$ . Then, we can find a linear head  $W \in \mathbb{R}^{m \times k}$  with small downstream error, that is,

$$\mathbb{E}_{x \sim p_{\text{data}}} [\|W \hat{f}(x) - e_{y(x)}\|_2^2] \leq 2rm\kappa^2 \rho^2. \quad (29)$$

On the other hand, suppose the positive-pair graph contains  $r_0$  disconnected clusters, and the function class is the set of universal function approximators  $\mathcal{F}_{\text{uni}}$ . So long as the output dimensionality  $k \leq \frac{1}{2} \cdot r_0$ , there exists solution  $\hat{f}' \in \arg \min_{f \in \mathcal{F}_{\text{uni}}} \mathcal{L}_\lambda(f)$  such that any linear head  $W \in \mathbb{R}^{m \times k}$  has bad test error, that is,

$$\mathbb{E}_{x \sim p_{\text{data}}} [\|W \hat{f}'(x) - e_{y(x)}\|_2^2] \geq \frac{1}{2}. \quad (30)$$

We note that a smaller  $\kappa$  (hence smoother function class) decreases the RHS of equation 29 and leads to better downstream performance. When  $r_0$  is much bigger than  $r$ , the above theorem shows that constraining the feature map to the Lipschitz continuous functions can allow for much smaller feature dimensionality. The proof of Theorem 5.9 is in Section D.3.

### 5.4 Convolutional neural networks

Our last example shows that convolutional neural networks can learn contrastive representation more efficiently than fully connected networks when the downstream task has a certain translational invariance structure. We consider the following data generative model where the data contains a patch that determines the downstream label.

**Example 5.10.** The natural data  $\bar{x} \in \mathbb{R}^d$  is defined as follows: for some location  $t \in [d]$  (which could depend on  $\bar{x}$ ) and consecutive  $s$  dimensions  $\bar{x}_{t:t+s-1}$  (the informative patch), we have  $\bar{x}_{t:t+s-1} \in \{-\gamma, \gamma\}^s$  where  $\gamma > 1$ .<sup>1</sup> The other  $d - s$  dimensions of  $\bar{x}$  (spurious dimensions) are all in  $\{-1, 1\}$ . Given a natural data  $\bar{x}$ , its augmentations are generated by the following procedure: for every spurious dimension  $i$ , first sample  $\tau_i \sim \text{Uni}[0, 1]$ , then multiply  $\bar{x}_i$  by  $\tau_i$ . The augmentation keeps the informative patch the same as original. The downstream task is a  $m$ -way classification problem such that the label function  $y(\cdot) : \mathcal{X} \rightarrow [m]$  satisfies  $y(x) = y(x')$  if the informative patches for  $x$  and  $x'$  are the same.

We consider the following convolutional neural network model with  $k$  channels.

**Definition 5.11** (Convolutional neural networks). Let  $U = [u_1, u_2, \dots, u_k]^\top \in \mathbb{R}^{k \times s}$  and  $b \in \mathbb{R}^k$ . We use  $f_{U,b}^{\text{conv}} : \mathcal{X} \rightarrow \mathbb{R}^k$  to represent the following convolutional neural network:  $f_{U,b}^{\text{conv}}(x)_i = \sum_{t=1}^d \sigma(u_i^\top x_{t:t+s-1} + b_i)$  where  $\sigma$  is ReLU activation function, and  $f_{U,b}^{\text{conv}}(x) = [f_{U,b}^{\text{conv}}(x)_1, \dots, f_{U,b}^{\text{conv}}(x)_k]^\top$ . We define the convolutional neural network class  $\mathcal{F}_{\text{conv}} = \{f_{U,b}^{\text{conv}} : U \in \mathbb{R}^{k \times s}, b \in \mathbb{R}^k\}$ .

Ideally, we would like to learn a feature map where the ReLU function is only activated on the informative patch. We have the following theorem which shows that contrastive learning with convolutional neural networks can indeed learn such ideal feature maps, hence allowing lower representation dimensionality than using fully-connected ReLU networks.

**Theorem 5.12.** In Example 5.10, let output dimensionality  $k = 2^s$  and learn a convolutional neural network  $\hat{f} \in \arg \min_{\mathcal{F}_{\text{conv}}} \mathcal{L}_\lambda(f)$  for some  $\lambda > 0$ . Then, we can find a linear head  $W \in \mathbb{R}^{m \times k}$  with zero downstream error, that is,

$$\mathbb{E}_{x \sim p_{\text{data}}} [\|W \hat{f}(x) - e_{y(x)}\|_2^2] = 0. \quad (31)$$

On the other hand, suppose the function class is the set of ReLU networks  $\mathcal{F}_{\text{ReLU}}$ , so long as the output dimensionality is less than  $d \times 2^{s-1}$ , there exists a function  $\hat{f}' \in \arg \min_{f \in \mathcal{F}_{\text{ReLU}}} \mathcal{L}_\lambda(f)$  such that any linear head  $W \in \mathbb{R}^{m \times k}$  has bad test error, that is,

$$\mathbb{E}_{x \sim p_{\text{data}}} [\|W \hat{f}'(x) - e_{y(x)}\|_2^2] \geq \frac{1}{2}. \quad (32)$$

When  $d \gg 2$ , the above theorem shows that constraining the feature map to convolutional networks can allow for much smaller feature dimensionality. The proof of Theorem 5.12 is in Section D.4.

## 6 Experiments

Recall that our assumptions intuitively state that the model architecture cannot break the data into *too many* well-separated clusters. In this section, we propose a method to empirically test how many clusters a model architecture can partition positive-pair graph of the data distribution into. Given a deep neural network and a target number of cluster  $r$ , ideally we aim to find a function  $f$  from the model class that maps each data point to a one-hot vector in dimension  $r$  which includes the cluster identity. That is,  $f(x) \in \{e_1, \dots, e_r\}$  where  $e_i$  is the  $i$ -th natural basis in  $\mathbb{R}^r$ . With this constraint, we minimize the disagreement between the functions outputs of a positive-pair, that is,  $\mathbb{E}_{(x, x^+) \sim p_{\text{pos}}} [\|f(x) - f(x^+)\|_2^2]$ , which compute the amount of inter-cluster edges. However, the one-hot vector requirement makes it challenging for optimization. Note that when the  $r$  clustering has

<sup>1</sup>Here we denote  $\bar{x}_{d+i} = \bar{x}_i$ .

the same probability mass  $1/r$ , we have  $\mathbb{E}[f(x)f(x)^\top] = \mathbb{I}/r$ . We use this equation as the constraint of  $f$  and arrive at a relaxation of the original optimization program.

$$b_r = \min \mathbb{E}_{(x,x^+) \sim p_{\text{pos}}} [\|f(x) - f(x^+)\|_2^2] \quad \text{s.t.} \quad \mathbb{E}[f(x)f(x)^\top] = \mathbb{I}/r \quad (33)$$

Thus, we use  $b_r$  as a surrogate for how the architecture can partition the graph into  $r$  clusters, and a smaller  $b_r$  means that it's easier to partition. We empirically implement equation 33 by first minimizing the contrastive loss  $\mathcal{L}_\lambda(f_\theta)$  with representation dimension  $k = r$  and a heavily-tuned regularization strength  $\lambda$ . Then, we whiten the obtained model  $f_{\hat{\theta}}(x)$  to have exactly the covariance  $\mathbb{I}/r$ , that is,  $\bar{f}(x) = \mathbb{E}_{x \sim p_{\text{data}}} [f_{\hat{\theta}}(x)f_{\hat{\theta}}(x)^\top]^{-\frac{1}{2}} f_{\hat{\theta}}(x)/\sqrt{r}$  is a valid solution for the program in equation 33. We compute  $b_r = \mathbb{E}_{(x,x^+) \sim p_{\text{pos}}} [\|\bar{f}(x) - \bar{f}(x^+)\|_2^2]$ . We also try various choices of  $\lambda$  and pick the smallest result as the final value of the estimated  $b_r$ .

We run this test with a ResNet-18 model on CIFAR-10 and compute the  $b_r$  for  $r \in \{10, 100\}$  list the results the table below. Here we note that  $b_r$  increases from 0.127 to 0.204 as  $r$  increases from 10 to 100, suggesting that although the network can partition the data relatively well into 10 clusters, it cannot partition the data into 100 well-separated clusters, which supports our theoretical assumptions. We also run the same test with a ResNet-101 model, and get  $b_{10} = 0.035$  and  $b_{100} = 0.172$ . It's worth noting these numbers are smaller than that of ResNet-18, due to the fact that ResNet-101 is much more expressive hence does a better job at partitioning the positive-pair graph. It's worth noting that there's always a gap between  $r = 10$  and  $r = 100$  regardless of the architecture, and for ResNet-101 the gap is larger, which is consistent with its better empirical performance. More details can be found in Appendix A.

	$r = 10$	$r = 100$
ResNet-18	0.127	0.204
ResNet-101	0.035	0.172

Table 1: The empirical  $r$ -way separability  $b_r$  on CIFAR-10 dataset.

## 7 Conclusion

In this paper, we provide a theoretical analysis of contrastive learning that incorporates the inductive biases of the model class. We prove that contrastive learning with appropriate model architectures allows for lower representation dimensionality (hence better sample complexity), and instantiate this theory on several interesting examples. One open question is to allow for overparameterization, i.e., showing similar results when  $k > m$ . Under our current theoretical framework, the optimal features are the top eigenfunctions of the graph Laplacian, and the learned representation may omit some top eigenfunctions when  $k > m$  and get suboptimal downstream performance. To allow for a more flexible choice of  $k$ , we believe that additional assumptions on the structure of the function class need to be made. Another open question would be theoretically studying the role of inductive biases under more common contrastive losses (e.g., the InfoNCE loss (Oord et al., 2018)). Finally, we note that our work only concerns the inductive biases originating from the model architecture, whereas in practice the learned representations may also depend on the optimization method (Liu et al., 2022). Hence, one interesting future direction would be studying how the *implicit bias* introduced by the optimizer influences contrastive learning.

## Acknowledge

Toyota Research Institute provided funds to support this work.

## References

- Sanjeev Arora, Hrishikesh Khandeparkar, Mikhail Khodak, Orestis Plevrakis, and Nikunj Saunshi. A theoretical analysis of contrastive unsupervised representation learning. In *International Conference on Machine Learning*, 2019.
- Jordan Ash, Surbhi Goel, Akshay Krishnamurthy, and Dipendra Misra. Investigating the role of negatives in contrastive representation learning. In *International Conference on Artificial Intelligence and Statistics*, pages 7187–7209. PMLR, 2022.
- Philip Bachman, R Devon Hjelm, and William Buchwalter. Learning representations by maximizing mutual information across views. *arXiv preprint arXiv:1906.00910*, 2019.
- Randall Balestriero and Yann LeCun. Contrastive and non-contrastive self-supervised learning recover global and local spectral embedding methods. *arXiv preprint arXiv:2205.11508*, 2022.
- Adrien Bardes, Jean Ponce, and Yann LeCun. Vicreg: Variance-invariance-covariance regularization for self-supervised learning. *arXiv preprint arXiv:2105.04906*, 2021.
- Tom Brown, Benjamin Mann, Nick Ryder, Melanie Subbiah, Jared D Kaplan, Prafulla Dhariwal, Arvind Neelakantan, Pranav Shyam, Girish Sastry, Amanda Askell, et al. Language models are few-shot learners. *Advances in neural information processing systems*, 33:1877–1901, 2020.
- Mathilde Caron, Ishan Misra, Julien Mairal, Priya Goyal, Piotr Bojanowski, and Armand Joulin. Unsupervised learning of visual features by contrasting cluster assignments. *arXiv preprint arXiv:2006.09882*, 33:9912–9924, 2020.
- Ting Chen, Simon Kornblith, Mohammad Norouzi, and Geoffrey Hinton. A simple framework for contrastive learning of visual representations. In *International Conference on Machine Learning (ICML)*, pages 1597–1607, 2020a.
- Ting Chen, Simon Kornblith, Mohammad Norouzi, and Geoffrey Hinton. A simple framework for contrastive learning of visual representations. In *International conference on machine learning*, volume 119 of *Proceedings of Machine Learning Research*, pages 1597–1607. PMLR, PMLR, 13–18 Jul 2020b.
- Ting Chen, Simon Kornblith, Kevin Swersky, Mohammad Norouzi, and Geoffrey Hinton. Big self-supervised models are strong semi-supervised learners. *arXiv preprint arXiv:2006.10029*, 2020c.
- Xinlei Chen and Kaiming He. Exploring simple siamese representation learning. *arXiv preprint arXiv:2011.10566*, pages 15750–15758, June 2020.
- Xinlei Chen and Kaiming He. Exploring simple siamese representation learning. In *Proceedings of the IEEE/CVF Conference on Computer Vision and Pattern Recognition*, pages 15750–15758, 2021.
- Xinlei Chen, Haoqi Fan, Ross Girshick, and Kaiming He. Improved baselines with momentum contrastive learning. *arXiv preprint arXiv:2003.04297*, 2020d.
- Alex Damian, Tengyu Ma, and Jason Lee. Label noise sgd provably prefers flat global minimizers, 2021.



- Alexey Dosovitskiy, Lucas Beyer, Alexander Kolesnikov, Dirk Weissenborn, Xiaohua Zhai, Thomas Unterthiner, Mostafa Dehghani, Matthias Minderer, Georg Heigold, Sylvain Gelly, et al. An image is worth 16x16 words: Transformers for image recognition at scale. In *International Conference on Learning Representations*, 2020.
- Yann Dubois, Tatsunori Hashimoto, Stefano Ermon, and Percy Liang. Improving self-supervised learning by characterizing idealized representations. *arXiv preprint arXiv:2209.06235*, 2022.
- Pierre Foret, Ariel Kleiner, Hossein Mobahi, and Behnam Neyshabur. Sharpness-aware minimization for efficiently improving generalization. *arXiv preprint arXiv:2010.01412*, 2020.
- Tianyu Gao, Xingcheng Yao, and Danqi Chen. Simcse: Simple contrastive learning of sentence embeddings. *arXiv preprint arXiv:2104.08821*, 2021.
- Quentin Garrido, Yubei Chen, Adrien Bardes, Laurent Najman, and Yann Lecun. On the duality between contrastive and non-contrastive self-supervised learning. *arXiv preprint arXiv:2206.02574*, 2022.
- Jeff Z. HaoChen, Colin Wei, Adrien Gaidon, and Tengyu Ma. Provable guarantees for self-supervised deep learning with spectral contrastive loss. *Advances in Neural Information Processing Systems*, 34:5000–5011, 2021.
- Jeff Z. HaoChen, Colin Wei, Ananya Kumar, and Tengyu Ma. Beyond separability: Analyzing the linear transferability of contrastive representations to related subpopulations. *Advances in Neural Information Processing Systems*, 2022.
- Kaiming He, Xiangyu Zhang, Shaoqing Ren, and Jian Sun. Deep residual learning for image recognition. In *arXiv preprint arXiv:1506.01497*, 2015.
- Kaiming He, Haoqi Fan, Yuxin Wu, Saining Xie, and Ross Girshick. Momentum contrast for unsupervised visual representation learning. In *Proceedings of the IEEE/CVF Conference on Computer Vision and Pattern Recognition*, pages 9729–9738, June 2020.
- Olivier Henaff. Data-efficient image recognition with contrastive predictive coding. In *International Conference on Machine Learning*, pages 4182–4192. PMLR, 2020.
- R Devon Hjelm, Alex Fedorov, Samuel Lavoie-Marchildon, Karan Grewal, Phil Bachman, Adam Trischler, and Yoshua Bengio. Learning deep representations by mutual information estimation and maximization. In *International Conference on Learning Representations*, 2018.
- Yiding Jiang, Behnam Neyshabur, Hossein Mobahi, Dilip Krishnan, and Samy Bengio. Fantastic generalization measures and where to find them. *arXiv preprint arXiv:1912.02178*, 2019.
- Michel Ledoux and Michel Talagrand. *Probability in Banach Spaces: isoperimetry and processes*, volume 23. Springer Science & Business Media, 1991.
- Jason D Lee, Qi Lei, Nikunj Saunshi, and Jiacheng Zhuo. Predicting what you already know helps: Provable self-supervised learning. *arXiv preprint arXiv:2008.01064*, 2020.
- Zhiyuan Li, Tianhao Wang, and Sanjeev Arora. What happens after sgd reaches zero loss?—a mathematical framework. *arXiv preprint arXiv:2110.06914*, 2021.
- Hong Liu, Sang Michael Xie, Zhiyuan Li, and Tengyu Ma. Same pre-training loss, better downstream: Implicit bias matters for language models. 2022.

- Ishan Misra and Laurens van der Maaten. Self-supervised learning of pretext-invariant representations. In *Proceedings of the IEEE/CVF Conference on Computer Vision and Pattern Recognition*, pages 6707–6717, 2020.
- Andrew Ng, Michael Jordan, and Yair Weiss. On spectral clustering: Analysis and an algorithm. *Advances in neural information processing systems*, 14:849–856, 2001.
- Kento Nozawa and Issei Sato. Understanding negative samples in instance discriminative self-supervised representation learning. *Advances in Neural Information Processing Systems*, 34:5784–5797, 2021.
- Aaron van den Oord, Yazhe Li, and Oriol Vinyals. Representation learning with contrastive predictive coding. *arXiv:1807.03748*, 2018.
- Alec Radford, Jeffrey Wu, Rewon Child, David Luan, Dario Amodei, Ilya Sutskever, et al. Language models are unsupervised multitask learners. *OpenAI blog*, 1(8):9, 2019.
- Joshua David Robinson, Ching-Yao Chuang, Suvrit Sra, and Stefanie Jegelka. Contrastive learning with hard negative samples. In *ICLR*, 2021.
- Nikunj Saunshi, Sadhika Malladi, and Sanjeev Arora. A mathematical exploration of why language models help solve downstream tasks. *arXiv preprint arXiv:2010.03648*, 2020.
- Nikunj Saunshi, Jordan Ash, Surbhi Goel, Dipendra Misra, Cyril Zhang, Sanjeev Arora, Sham Kakade, and Akshay Krishnamurthy. Understanding contrastive learning requires incorporating inductive biases. *arXiv preprint arXiv:2202.14037*, 2022.
- Jianbo Shi and Jitendra Malik. Normalized cuts and image segmentation. *IEEE Transactions on pattern analysis and machine intelligence*, 22(8):888–905, 2000.
- Yixuan Su, Fangyu Liu, Zaiqiao Meng, Tian Lan, Lei Shu, Ehsan Shareghi, and Nigel Collier. *Tacl: Improving bert pre-training with token-aware contrastive learning*, 2021.
- Yonglong Tian, Dilip Krishnan, and Phillip Isola. Contrastive multiview coding. *arXiv preprint arXiv:1906.05849*, 2019.
- Yonglong Tian, Chen Sun, Ben Poole, Dilip Krishnan, Cordelia Schmid, and Phillip Isola. What makes for good views for contrastive learning. *arXiv preprint arXiv:2005.10243*, 2020.
- Yuandong Tian. Deep contrastive learning is provably (almost) principal component analysis. *arXiv preprint arXiv:2201.12680*, 2022.
- Yuandong Tian, Xinlei Chen, and Surya Ganguli. Understanding self-supervised learning dynamics without contrastive pairs. In *International Conference on Machine Learning*, pages 10268–10278. PMLR, 2021.
- Christopher Tosh, Akshay Krishnamurthy, and Daniel Hsu. Contrastive estimation reveals topic posterior information to linear models. *arXiv:2003.02234*, 2020.
- Christopher Tosh, Akshay Krishnamurthy, and Daniel Hsu. Contrastive learning, multi-view redundancy, and linear models. In *Algorithmic Learning Theory*, pages 1179–1206. PMLR, 2021.
- Luca Trevisan. Notes on expansion , sparsest cut , and spectral graph theory. 2015.

- Luca Trevisan. Lecture notes on graph partitioning, expanders and spectral methods. *University of California, Berkeley*, <https://people.eecs.berkeley.edu/luca/books/expanders-2016.pdf>, 2017.
- Yifei Wang, Qi Zhang, Yisen Wang, Jiansheng Yang, and Zhouchen Lin. Chaos is a ladder: A new theoretical understanding of contrastive learning via augmentation overlap. In *International Conference on Learning Representations*, 2021.
- Colin Wei and Tengyu Ma. Data-dependent sample complexity of deep neural networks via lipschitz augmentation. In *Advances in Neural Information Processing Systems*, pages 9722–9733, 2019.
- Colin Wei and Tengyu Ma. Improved sample complexities for deep networks and robust classification via an all-layer margin. In *International Conference on Learning Representations (ICLR)*, 2020.
- Colin Wei, Sang Michael Xie, and Tengyu Ma. Why do pretrained language models help in downstream tasks? an analysis of head and prompt tuning. *Advances in Neural Information Processing Systems*, 34:16158–16170, 2021.
- Zixin Wen and Yuanzhi Li. Toward understanding the feature learning process of self-supervised contrastive learning. In *International Conference on Machine Learning*, pages 11112–11122. PMLR, 2021.
- Zixin Wen and Yuanzhi Li. The mechanism of prediction head in non-contrastive self-supervised learning. *arXiv preprint arXiv:2205.06226*, 2022.
- Zhirong Wu, Yuanjun Xiong, Stella X Yu, and Dahua Lin. Unsupervised feature learning via non-parametric instance discrimination. In *Proceedings of the IEEE Conference on Computer Vision and Pattern Recognition*, pages 3733–3742, 2018.
- Sang Michael Xie, Aditi Raghunathan, Percy Liang, and Tengyu Ma. An explanation of in-context learning as implicit bayesian inference. In *International Conference on Learning Representations*, 2021.
- Mang Ye, Xu Zhang, Pong C Yuen, and Shih-Fu Chang. Unsupervised embedding learning via invariant and spreading instance feature. In *Proceedings of the IEEE/CVF Conference on Computer Vision and Pattern Recognition*, pages 6210–6219, 2019.
- Jure Zbontar, Li Jing, Ishan Misra, Yann LeCun, and Stéphane Deny. Barlow twins: Self-supervised learning via redundancy reduction. In *International Conference on Machine Learning*, pages 12310–12320. PMLR, 2021.

## A Addition experimental details

We train a ResNet-18 model on CIFAR-10 training set and test the  $b_r$  on the test set. We train with SGD using initial learning rate 0.01 and decays with cosine schedule. All experiments are run for 200 epochs. We test with  $r \in \{10, 100, 500\}$  and grid search using  $\lambda \in \{0.1, 0.3, 1, 3, 10, 30, 100, 300, 1000\}$ , the result for each configurate is listed in the table below.

$\lambda$	0.1	0.3	1	3	10	30	100	300	1000
$r = 10$	0.445	<b>0.127</b>	0.134	0.144	0.151	0.155	0.215	0.343	0.901
$r = 100$	0.887	0.660	0.408	0.245	<b>0.204</b>	0.220	0.254	0.424	1.579
$r = 500$	1.031	0.981	0.710	0.554	0.427	0.372	<b>0.315</b>	0.481	1.231

We also report the result for ResNet101 on CIFAR-10, listed as follows:

$\lambda$	0.1	0.3	1	3	10	30	100	300	1000
$r = 10$	1.270	<b>0.035</b>	0.045	0.057	0.066	0.077	0.091	0.088	0.144
$r = 100$	1.044	1.255	0.643	0.312	<b>0.172</b>	0.213	0.358	1.804	1.912

## B Proofs for Section 3

*Proof of Theorem 3.6.* Let  $P_i := \Pr_{x \sim p_{\text{data}}}(x \in S_i)$  be the probability of  $S_i$ . Let  $f^*$  be the function  $f^*(x) = \frac{1}{\sqrt{P_{\text{id}_x}}} e_{\text{id}_x}$ . From Assumption 3.4 and Assumption 3.5, we have  $f^* \in \mathcal{F}$ .

We first show that  $f^*$  achieve small contrastive loss. For the regularizer term, we have

$$\mathbb{E}_{x \sim p_{\text{data}}} \left[ f^*(x) f^*(x)^\top \right] = \sum_{i \in [m]} P_i \cdot \frac{1}{P_i} \cdot e_{\text{id}_x} e_{\text{id}_x}^\top = \mathbb{I}. \quad (34)$$

Thus, we have  $R(f^*) = 0$ . For the discrepancy term, let  $P_{\min} := \min_{i \in [m]} P_i$  be the probability mass of the smallest set, we have

$$\mathbb{E}_{x, x^+} \left[ \|f^*(x) - f^*(x^+)\|_2^2 \right] \leq \frac{1}{P_{\min}} \cdot \Pr_{(x, x^+) \sim p_{\text{pos}}} (\text{id}_x \neq \text{id}_{x^+}) \leq \frac{\alpha}{P_{\min}}. \quad (35)$$

Combining equation 34 and equation 35 we have

$$\mathcal{L}_\lambda(f^*) = \mathbb{E}_{x, x^+} \left[ \|f^*(x) - f^*(x^+)\|_2^2 \right] + \lambda \cdot R(f) \leq \frac{\alpha}{P_{\min}}. \quad (36)$$

Since  $\hat{f} = \arg \min_{f \in \mathcal{F}} \mathcal{L}_\lambda(f)$  is the minimizer of contrastive loss within the function class, we have

$$\mathcal{L}_\lambda(\hat{f}) \leq \mathcal{L}_\lambda(f^*) \leq \frac{\alpha}{P_{\min}}. \quad (37)$$

Define matrix

$$M := \mathbb{E}_{x \sim p_{\text{data}}} \left[ \hat{f}(x) \hat{f}(x)^\top \right]. \quad (38)$$

We have

$$\|M - \mathbb{I}\|_F^2 \leq \frac{\mathcal{L}_\lambda(\hat{f})}{\lambda} \leq \frac{\alpha}{\lambda P_{\min}}. \quad (39)$$

Since  $\lambda > \frac{\alpha}{P_{\min}}$ , we know that  $M$  is a full rank matrix, thus we can define function

$$\tilde{f}(x) := M^{-\frac{1}{2}} \hat{f}(x). \quad (40)$$

Let

$$Q := \mathbb{E}_{x \sim p_{\text{data}}} \left[ \tilde{f}(x) f^*(x)^\top \right], \quad (41)$$

and

$$\pi_f(x) := \tilde{f}(x) - Q f^*(x). \quad (42)$$

We know that

$$\mathbb{E}_{x \sim p_{\text{data}}} \left[ \pi_f(x) f^*(x)^\top \right] = \mathbb{E}_{x \sim p_{\text{data}}} \left[ \tilde{f}(x) f^*(x)^\top \right] - Q \mathbb{E}_{x \sim p_{\text{data}}} \left[ f^*(x) f^*(x)^\top \right] = 0. \quad (43)$$

Using Assumption 3.3 we have:

$$\begin{aligned} & \mathbb{E}_{(x, x^+) \sim p_{\text{pos}}} \left[ \|\pi_f(x) - \pi_f(x^+)\|_2^2 \right] \\ & \geq \sum_{i \in [m]} (P_i - \alpha) \cdot \mathbb{E}_{(x, x^+) \sim p_{\text{pos}_i}} \left[ \|\pi_f(x) - \pi_f(x^+)\|_2^2 \right] \\ & \geq \beta \cdot \sum_{i \in [m]} (P_i - \alpha) \cdot \mathbb{E}_{x \sim p_{\text{data}_i}, x' \sim p_{\text{data}_i}} \left[ \|\pi_f(x) - \pi_f(x')\|_2^2 \right] \\ & = 2\beta \cdot \sum_{i \in [m]} (P_i - \alpha) \cdot \mathbb{E}_{x \sim p_{\text{data}_i}} \left[ \|\pi_f(x)\|_2^2 \right] \\ & = 2\beta \cdot \left(1 - \frac{\alpha}{P_{\min}}\right) \cdot \mathbb{E}_{x \sim p_{\text{data}}} \left[ \|\pi_f(x)\|_2^2 \right]. \end{aligned} \quad (44)$$

On the other hand, we have

$$\begin{aligned} & \mathbb{E}_{(x, x^+) \sim p_{\text{pos}}} \left[ \|\pi_f(x) - \pi_f(x^+)\|_2^2 \right] \\ & \leq \mathbb{E}_{(x, x^+) \sim p_{\text{pos}}} \left[ \|\tilde{f}(x) - \tilde{f}(x^+)\|_2^2 \right] \\ & \leq \|M^{-1}\|_{\text{spec}} \cdot \mathbb{E}_{(x, x^+) \sim p_{\text{pos}}} \left[ \|\hat{f}(x) - \hat{f}(x^+)\|_2^2 \right] \\ & \leq \left(1 + \sqrt{\frac{\alpha}{\lambda P_{\min}}}\right) \cdot \frac{\alpha}{P_{\min}}. \end{aligned} \quad (45)$$

Combining equation 44 and equation 45 we have

$$\mathbb{E}_{x \sim p_{\text{data}}} \left[ \|\pi_f(x)\|_2^2 \right] \leq \left(1 + \sqrt{\frac{\alpha}{\lambda P_{\min}}}\right) \cdot \frac{\alpha}{2\beta(P_{\min} - \alpha)}. \quad (46)$$

By Lemma B.1, we know that there exists a matrix  $U \in \mathbb{R}^{m \times m}$  such that

$$\mathbb{E}_{x \sim p_{\text{data}}} \left[ \left\| f^*(x) - U M^{-1/2} \hat{f}(x) \right\|_2^2 \right] \leq \left(1 + \sqrt{\frac{\alpha}{\lambda P_{\min}}}\right) \cdot \frac{\alpha}{2\beta(P_{\min} - \alpha)} \quad (47)$$

$$\leq \frac{\alpha}{\beta(P_{\min} - \alpha)}. \quad (48)$$

Thus, if we define matrix  $W = \text{diag}\{\sqrt{P_1}, \sqrt{P_2}, \dots, \sqrt{P_m}\}UM^{-1/2}$ , then we have

$$\mathbb{E}_{x \sim p_{\text{data}}} \left[ \left\| e_{\text{id}_x} - W \hat{f}(x) \right\|_2^2 \right] \leq P_{\max} \mathbb{E}_{x \sim p_{\text{data}}} \left[ \left\| f^*(x) - UM^{-1/2} \hat{f}(x) \right\|_2^2 \right] \quad (49)$$

$$\leq P_{\max} \frac{\alpha}{\beta(P_{\min} - \alpha)}, \quad (50)$$

which finishes the proof. □

**Lemma B.1.** Suppose  $f : \mathcal{X} \rightarrow \mathbb{R}^m$  and  $g : \mathcal{X} \rightarrow \mathbb{R}^m$  are two functions defined on  $\mathcal{X}$  such that

$$\mathbb{E}_{x \sim p_{\text{data}}} \left[ f(x) f(x)^\top \right] = \mathbb{E}_{x \sim p_{\text{data}}} \left[ g(x) g(x)^\top \right] = \mathbb{I}. \quad (51)$$

Define the projection of  $f$  onto  $g$ 's orthogonal subspace as:

$$\pi_f(x) = f(x) - \mathbb{E}_{x' \sim p_{\text{data}}} \left[ f(x) g(x)^\top \right] g(x). \quad (52)$$

Then, there exists matrix  $U \in \mathbb{R}^{m \times m}$  such that

$$\mathbb{E}_{x \sim p_{\text{data}}} \left[ \|g(x) - Uf(x)\|_2^2 \right] = \mathbb{E}_{x \sim p_{\text{data}}} \left[ \|\pi_f(x)\|_2^2 \right]. \quad (53)$$

*Proof of Lemma B.1.* Let matrix

$$U = \mathbb{E}_{x' \sim p_{\text{data}}} \left[ g(x) f(x)^\top \right]. \quad (54)$$

We have

$$\mathbb{E}_{x \sim p_{\text{data}}} \left[ \|g(x) - Uf(x)\|_2^2 \right] \quad (55)$$

$$= \mathbb{E}_{x \sim p_{\text{data}}} \left[ \|g(x)\|_2^2 \right] - 2 \mathbb{E}_{x \sim p_{\text{data}}} \left[ g(x)^\top Uf(x) \right] + \mathbb{E}_{x \sim p_{\text{data}}} \left[ f(x)^\top U^\top Uf(x) \right] \quad (56)$$

$$= m - 2 \|U\|_F^2 + \|U\|_F^2 \quad (57)$$

$$= m - \|U\|_F^2. \quad (58)$$

On the other hand, we have

$$\mathbb{E}_{x \sim p_{\text{data}}} \left[ \|\pi_f(x)\|_2^2 \right] \quad (59)$$

$$= \mathbb{E}_{x \sim p_{\text{data}}} \left[ \left\| f(x) - U^\top g(x) \right\|_2^2 \right] \quad (60)$$

$$= \mathbb{E}_{x \sim p_{\text{data}}} \left[ \|f(x)\|_2^2 \right] - 2 \mathbb{E}_{x \sim p_{\text{data}}} \left[ f(x)^\top U^\top g(x) \right] + \mathbb{E}_{x \sim p_{\text{data}}} \left[ g(x)^\top U U^\top g(x) \right] \quad (61)$$

$$= m - \|U\|_F^2. \quad (62)$$

Thus, we have

$$\mathbb{E}_{x \sim p_{\text{data}}} \left[ \|g(x) - Uf(x)\|_2^2 \right] = \mathbb{E}_{x \sim p_{\text{data}}} \left[ \|\pi_f(x)\|_2^2 \right], \quad (63)$$

which finishes the proof. □

## C Proofs for Section 4

*Proof of Proposition 4.1.* Define function

$$\tilde{g}(x) = \sqrt{p_{\text{data}}(x)}g(x). \quad (64)$$

Define the symmetric Laplacian operator

$$\tilde{\mathbb{L}}(\tilde{g})(x) = \tilde{g}(x) - \int \frac{p_{\text{pos}}(x, x')}{\sqrt{p_{\text{data}}(x)}\sqrt{p_{\text{data}}(x')}}\tilde{g}(x')dx'. \quad (65)$$

It can be verified that

$$\int_x \tilde{g}(x)\tilde{\mathbb{L}}(\tilde{g})(x) = 0. \quad (66)$$

Notice that the operator  $\tilde{\mathbb{L}}$  is PSD, we have that

$$\int_x (\tilde{\mathbb{L}}(\tilde{g})(x))^2 = 0, \quad (67)$$

which is equivalent to

$$\mathbb{E}_{x \sim p_{\text{data}}} [(\mathbb{L}(\tilde{g})(x))^2] = 0, \quad (68)$$

hence finishes the proof.  $\square$

*Proof of Theorem 4.4.* Notice that  $\mathcal{L}_\lambda(f_{\text{eig}}) \leq \phi$ , we know that  $\mathcal{L}_\lambda(\hat{f}) \leq \phi$ , so

$$\left\| \mathbb{E}_{x \sim p_{\text{data}}} [\hat{f}(x)\hat{f}(x)^\top] - \mathbb{I} \right\|_F^2 \leq \frac{\phi}{\lambda}, \quad (69)$$

and

$$\mathbb{E}_{(x, x^+) \sim p_{\text{pos}}} \left[ \left\| \hat{f}(x) - \hat{f}(x^+) \right\|_2^2 \right] \leq \phi. \quad (70)$$

Therefore, for any  $i \in [k]$ , we have

$$\mathbb{E}_{x \sim p_{\text{data}}} [\hat{f}(x)_i^2] \geq 1 - \sqrt{\frac{\phi}{\lambda}}, \quad (71)$$

and

$$\mathbb{E}_{(x, x^+) \sim p_{\text{pos}}} \left[ \left( \hat{f}(x)_i - \hat{f}(x^+)_i \right)^2 \right] \leq \phi. \quad (72)$$

Thus,

$$\mathbb{E}_{(x, x^+) \sim p_{\text{pos}}} \left[ \left( \hat{f}(x)_i - \hat{f}(x^+)_i \right)^2 \right] \leq \frac{\phi}{1 - \sqrt{\frac{\phi}{\lambda}}} \cdot \mathbb{E}_{x \sim p_{\text{data}}} [\hat{f}(x)_i^2] \leq \tilde{\phi} \cdot \mathbb{E}_{x \sim p_{\text{data}}} [\hat{f}(x)_i^2]. \quad (73)$$

In Assumption 4.2, set  $g = \hat{f}_i$  and sum over  $i = 1, 2, \dots, k$ , we have that for some matrix  $\tilde{W}$ ,

$$\mathbb{E}_{x \sim p_{\text{data}}} \left[ \left\| \tilde{W} f_{\text{eig}}(x) - \hat{f}(x) \right\|_2^2 \right] \leq k\epsilon. \quad (74)$$

Let matrix  $Q := \mathbb{E}_{x \sim p_{\text{data}}} [\hat{f}(x)\hat{f}(x)^\top]$ , we have that

$$\mathbb{E}_{x \sim p_{\text{data}}} \left[ \left\| Q^{-1/2} \hat{f}(x) - \hat{f}(x) \right\|_2^2 \right] \leq \frac{2\phi}{\lambda} \cdot \mathbb{E}_{x \sim p_{\text{data}}} \left[ \left\| \hat{f}(x) \right\|_2^2 \right] \leq \frac{2\phi}{\lambda} k \left( 1 + \sqrt{\frac{\phi}{\lambda}} \right). \quad (75)$$

Thus,

$$\mathbb{E}_{x \sim p_{\text{data}}} \left[ \left\| \tilde{W} f_{\text{eig}}(x) - Q^{-1/2} \hat{f}(x) \right\|_2^2 \right] \leq 2k\epsilon + \frac{4\phi}{\lambda} k \left( 1 + \sqrt{\frac{\phi}{\lambda}} \right). \quad (76)$$

Define matrix

$$M := \mathbb{E}_{x \sim p_{\text{data}}} \left[ f_{\text{eig}}(x) \hat{f}(x)^\top Q^{-1/2} \right] \quad (77)$$

Using Lemma B.1 and equation 76 we have

$$\mathbb{E}_{x \sim p_{\text{data}}} \left[ \left\| f_{\text{eig}}(x) - MQ^{-1/2} \hat{f}(x) \right\|_2^2 \right] \leq 2k\epsilon + \frac{4\phi}{\lambda} k \left( 1 + \sqrt{\frac{\phi}{\lambda}} \right) \leq 2k\epsilon + \frac{8\phi}{\lambda} k. \quad (78)$$

Thus, using Assumption 4.3, we have

$$\mathbb{E}_{x \sim p_{\text{data}}} \left[ \left\| W^* MQ^{-1/2} \hat{f}(x) - e_{y(x)} \right\|_2^2 \right] \quad (79)$$

$$\leq 2\mathbb{E}_{x \sim p_{\text{data}}} \left[ \left\| W^* f_{\text{eig}}(x) - e_{y(x)} \right\|_2^2 \right] + 2\mathbb{E}_{x \sim p_{\text{data}}} \left[ \left\| W^* MQ^{-1/2} \hat{f}(x) - W^* f_{\text{eig}}(x) \right\|_2^2 \right] \quad (80)$$

$$\leq 2\zeta + 4B^2 k\epsilon + \frac{16\phi}{\lambda} B^2 k. \quad (81)$$

□

### C.1 Proof for Section 4.1

*Proof of Theorem 4.6.* We first show that with high probability,  $\mathcal{L}_\lambda(\hat{f})$  is small. Consider the following decomposition

$$\mathcal{L}_\lambda(f) - \hat{\mathcal{L}}_\lambda(f) = T_1 + T_2 + T_3, \quad (82)$$

where

$$T_1 = \mathbb{E} \left[ \left\| f(x) - f(x^+) \right\|^2 \right] - \hat{\mathbb{E}} \left[ \left\| f(x) - f(x^+) \right\|^2 \right], \quad (83)$$

$$T_2 = \lambda \text{Tr} \left( \mathbb{E} \left[ f(x) f(x)^\top \right]^2 - \hat{\mathbb{E}} \left[ f(x) f(x)^\top \right]^2 \right), \quad (84)$$

$$T_3 = -2\lambda \left( \text{Tr} \left( \mathbb{E} \left[ f(x) f(x)^\top \right] \right) - \text{Tr} \left( \hat{\mathbb{E}} \left[ f(x) f(x)^\top \right] \right) \right). \quad (85)$$

Here we use  $\mathbb{E}$  to denote expectation over population distribution, and  $\hat{\mathbb{E}}$  to denote expectation over the empirical dataset. Since  $\|f(x) - f(x^+)\|^2 \leq 4C_f^2$ , using the uniform convergence bound via Rademacher complexity and Talagrand's Contraction Lemma (Ledoux and Talagrand, 1991), we have that with probability at least  $1 - \frac{\delta}{6}$ ,

$$T_1 \leq 8C_f \hat{\mathcal{R}}_{n_{\text{pre}}}(\mathcal{F}) + 4C_f^2 \sqrt{\frac{\log(6/\delta)}{2n_{\text{pre}}}}. \quad (86)$$

Notice that

$$T_2 \leq 2C_f^2 \lambda \cdot \sum_{i,j} \left| \mathbb{E} [f(x)_i f(x)_j] - \hat{\mathbb{E}} [f(x)_i f(x)_j] \right|, \quad (87)$$



we have that with probability at least  $1 - \frac{\delta}{6}$ ,

$$T_2 \leq 2C_f^2 \lambda k^2 \cdot C_f \widehat{\mathcal{R}}_{n_{\text{pre}}}(\mathcal{F}) + 2C_f^2 \lambda k^2 \cdot 2C_f^2 \sqrt{\frac{\log(6k^2/\delta)}{2n_{\text{pre}}}}. \quad (88)$$

Notice that

$$T_3 \leq 2\lambda \cdot \left| \mathbb{E} [\|f(x)_2^2\|] - \widehat{\mathbb{E}} [\|f(x)^2\|] \right|, \quad (89)$$

we have that with probability at least  $1 - \frac{\delta}{6}$ ,

$$T_3 \leq 2\lambda \cdot C_f \widehat{\mathcal{R}}_{n_{\text{pre}}}(\mathcal{F}) + 2\lambda \cdot C_f^2 \sqrt{\frac{\log(6/\delta)}{2n_{\text{pre}}}}. \quad (90)$$

Thus, with probability at least  $1 - \frac{\delta}{2}$ , we have the following inequality for all  $f \in \mathcal{F}$ :

$$\mathcal{L}_\lambda(f) - \widehat{\mathcal{L}}_\lambda(f) \leq (8C_f + 2C_f^3 \lambda k^2 + 2C_f \lambda) \cdot \widehat{\mathcal{R}}_{n_{\text{pre}}}(\mathcal{F}) + (4C_f^2 + 4C_f^4 \lambda k^2 + 2C_f^2 \lambda) \cdot \sqrt{\frac{\log(6k^2/\delta)}{2n_{\text{pre}}}}. \quad (91)$$

When the RHS of equation 91 (which we refer as ‘‘RHS’’ below) is smaller than  $\frac{1}{2}\tilde{\phi} - \phi$ , we have that

$$\mathcal{L}_\lambda(\hat{f}) \leq \phi + \text{RHS} \leq \frac{1}{2}\tilde{\phi}. \quad (92)$$

Thus, following the same proof as Theorem 4.4, we know that there exists a linear head  $W \in \mathbb{R}^{r \times k}$  defined as

$$W = W^* \cdot \mathbb{E}_{x \sim p_{\text{data}}} [f_{\text{eig}}(x) \hat{f}(x)^\top] \cdot \mathbb{E}_{x \sim p_{\text{data}}} [\hat{f}(x) \hat{f}(x)^\top]^{-1}, \quad (93)$$

such that

$$\mathbb{E}_{x \sim p_{\text{data}}} [\|W \hat{f}(x) - \vec{y}(x)\|_2^2] \leq 2\zeta + 4B^2 k \epsilon + \frac{4(\phi + \text{RHS})}{\lambda} B^2 k. \quad (94)$$

Since  $\lambda > 2\tilde{\phi}$ , we have  $\|\mathbb{E}_{x \sim p_{\text{data}}} [\hat{f}(x) \hat{f}(x)^\top]^{-1}\|_2 \leq 2$  and  $\|\mathbb{E}_{x \sim p_{\text{data}}} [f_{\text{eig}}(x) \hat{f}(x)^\top]\|_2 \leq 2$ , thus  $\|W\|_F \leq 4B$ . Using uniform convergence bound again, we have that with probability at least  $1 - \frac{\delta}{2}$ ,

$$\mathbb{E}_{x \sim p_{\text{data}}} [\|\widehat{W} \hat{f}(x) - \vec{y}(x)\|_2^2] \lesssim \zeta + B^2 k (\epsilon + \frac{\phi + \text{RHS}}{\lambda}) + BC_f \cdot \sqrt{\frac{\log(1/\delta)}{n_{\text{ds}}}}. \quad (95)$$

Since  $\widehat{W} = 0$  gives trivial test loss 1, we can add an additional term to equation 95 to also cover the case when the RHS of equation 91 is larger than  $\frac{1}{2}\tilde{\phi} - \phi$ , as follows:

$$\mathbb{E}_{x \sim p_{\text{data}}} [\|\widehat{W} \hat{f}(x) - \vec{y}(x)\|_2^2] \quad (96)$$

$$\lesssim \zeta + B^2 k (\epsilon + \frac{\phi + \text{RHS}}{\lambda}) + \frac{C_f^4 k^2 \lambda}{\tilde{\phi} - 2\phi} \left( \widehat{\mathcal{R}}_{n_{\text{pre}}}(\mathcal{F}) + \sqrt{\frac{\log(k^2/\delta)}{n_{\text{pre}}}} \right) + BC_f \sqrt{\frac{\log(1/\delta)}{n_{\text{ds}}}} \quad (97)$$

$$\lesssim \zeta + B^2 k (\epsilon + \frac{\phi}{\lambda}) + \frac{C_f^4 k^2 \lambda + B^2 k}{\tilde{\phi} - 2\phi} \left( \widehat{\mathcal{R}}_{n_{\text{pre}}}(\mathcal{F}) + \sqrt{\frac{\log(k^2/\delta)}{n_{\text{pre}}}} \right) + BC_f \sqrt{\frac{\log(1/\delta)}{n_{\text{ds}}}}, \quad (98)$$

where the second inequality uses  $\lambda > 2\tilde{\phi} > \tilde{\phi} - 2\phi$ .

□

## D Proofs for Section 5

### D.1 Proof for Example 5.1

*Proof of Theorem 5.3.* Define  $\hat{U} = [e_1, e_2, \dots, e_s]^\top \in \mathbb{R}^{s \times d}$ . We can verify that

$$\mathbb{E}_{(x, x^+) \sim p_{\text{pos}}} [\|f_{\hat{U}}(x) - f_{\hat{U}}(x^+)\|_2^2] = 0 \quad (99)$$

and

$$\mathbb{E}_{x \sim p_{\text{data}}} [f_{\hat{U}}(x) f_{\hat{U}}(x)^\top] = \mathbb{I}. \quad (100)$$

Thus, we can view  $f_{\hat{U}}$  as the  $f_{\text{eig}}$  in Section 4.

Let  $U \in \mathbb{R}^{k \times d}$  and  $i \in [k]$  such that

$$\mathbb{E}_{(x, x^+) \sim p_{\text{pos}}} [(f_U(x)_i - f_U(x^+)_i)^2] = 0. \quad (101)$$

Notice that  $x$  and  $x^+$  only differs on the  $s + 1$ -th to  $d$ -th dimensions, we know that  $U_i$  is 0 on the  $s + 1$ -th to  $d$ -th dimensions. Thus, we have that  $U_i$  is in the span of  $e_1, e_2, \dots, e_s$ , and as a result Assumption 4.2 holds with  $\epsilon = 0$ .

Since the downstream task's label is equal to  $x_i$  for  $i \in [s]$ , we can set  $W^* = e_i^\top$  and we would have

$$\mathbb{E}_{x \sim p_{\text{data}}} [(W^* f_U(x) - \bar{y}(x))^2] = 0. \quad (102)$$

Hence Assumption 4.3 holds with  $\alpha = 0$  and  $B = 1$ .

Applying Theorem 4.4 finishes the proof for the linear function class case.

For the case of universal function approximators, without loss of generality we assume the downstream task's label only depends on the first dimension of  $x$ , i.e.,  $y(x) = \text{sgn}(x_1)$ . When  $k \leq 2^{d-1}$ , we can construct a function  $f : \mathcal{X} \rightarrow \mathbb{R}^k$  such that for every dimension  $j \in [k]$ , we have  $f(x)_j = \sqrt{k}$  when  $x_{2:d}$  viewed as a binary number equals to  $j$ , otherwise  $f(x)_j = 0$ . It can be verified that  $\mathcal{L}_\lambda(f) = 0$  hence  $f$  is a minimizer of the contrastive loss. However,  $f(x)$  is agnostic to the first dimension of  $x$ , hence the downstream error is at least 1.  $\square$

### D.2 Proof for Example 5.4

*Proof of Theorem 5.6.* For any vector  $h \in \{-1, 1\}^s$ , we define function  $\text{bin}(h) \in \{0, 1, \dots, 2^s - 1\}$  be the function that maps  $h$  to the corresponding number when viewing  $\frac{1}{2}(h+1)$  as binary. Since  $\text{bin}(\cdot)$  is a one-to-one mapping, we can define  $U \in \{k \times d\}$  such that the  $i$ -th row of  $U$  satisfies: the first  $s$  dimensions equal to  $\sqrt{k} \cdot \text{bin}^{-1}(i-1)$ , and the rest  $d-s$  dimensions are 0. Let bias vector  $b \in \mathbb{R}^k$  such that every dimension is  $-\sqrt{k} \cdot (r-1)$ . We have  $f_{U,b}(x) = \sqrt{k} \cdot e_{\text{bin}(x_{1:s})+1} \in \mathbb{R}^k$ .

Since  $\mathbb{E}_{x \sim p_{\text{data}}} [f_{U,b}(x) f_{U,b}(x)^\top] = \mathbb{I}$  and  $\mathbb{E}_{(x, x^+) \sim p_{\text{pos}}} [\|f_{U,b}(x) - f_{U,b}(x^+)\|_2^2] = 0$ , we can view  $f_{U,b}$  as the  $f_{\text{eig}}$  in Section 4. Assumption 4.3 naturally hold with  $B = 1$ .

For Assumption 4.2, consider a function  $f_{U',b'} \in \mathcal{F}_{\text{ReLU}}$  and index  $i \in [k]$  such that  $\mathbb{E}_{(x, x^+) \sim p_{\text{pos}}} [(f_{U',b'}(x)_i - f_{U',b'}(x^+)_i)^2] = 0$ . Suppose there exist  $\bar{x} \neq \bar{x}'$  and their augmentations  $x, x'$  such that  $f_{U',b'}(x)_i > f_{U',b'}(x')_i$ . Then, there must be  $(U_i)_{r+1:d} \neq 0$  and  $\sigma(U_i^\top x) > 0$ . This suggests that there must exist another  $\tilde{x}$  which is also an augmentation of  $\bar{x}$  but  $\sigma(U_i^\top x) \neq \sigma(U_i^\top \tilde{x})$ . Hence, we have

$$\mathbb{E}_{(x, x^+) \sim p_{\text{pos}}} [(f_{U',b'}(x)_i - f_{U',b'}(x^+)_i)^2] > 0, \quad (103)$$

leading to contradiction. Hence, we know that  $f_{U',b'}(x)_i = f_{U',b'}(x')_i$ , so  $(f_{U',b'})_i$  can only be a function of  $x_{1:s}$ . Therefore, there exists a vector  $w \in \mathbb{R}^k$  such that  $f_{U',b'}(x)_i = w^\top f_{U,b}(x)$ , which means Assumption 4.2 holds with  $\epsilon = 0$ . Applying Theorem 4.4 finishes the proof for equation 27.

The result about universal function approximators follows the same proof as for Theorem 5.3 except for constructing the function using the last  $(d - s)$  dimensions rather than the last  $(d - 1)$  dimensions.  $\square$

### D.3 Proof for Example 5.7

*Proof of Theorem 5.9.* Let  $\text{id}_x$  be the index such that  $x \in S_{\text{id}_x}$ , and define function  $f_{\text{eig}}(x) = \sqrt{m} \cdot e_{\text{id}_x}$ . It can be verified that  $f_{\text{eig}}$  satisfies equation 15 and equation 16. For  $f \in \mathcal{F}_{\text{Lip},\kappa}$  and  $i \in [m]$ , define  $g(x) = f(x)_i$ . Suppose  $\mathbb{E}_{x \sim p_{\text{data}}}[g(x)^2] = 1$ , we can choose  $m$  data  $x_1, x_2, \dots, x_m$  such that  $x_i \in S_i$  and  $\frac{1}{m} \sum_{i \in [m]} g(x_i)^2 \leq 1$ . Define vector  $\tilde{w} \in \mathbb{R}^m$  such that  $\tilde{w}_i = \frac{1}{\sqrt{m}} \cdot g(x_i)$ . We have

$$\mathbb{E}_{x \sim p_{\text{data}}} \left[ (\tilde{w}^\top f_{\text{eig}}(x) - g(x))^2 \right] = \frac{1}{m} \sum_{i \in [m]} \mathbb{E}_{x \sim S_i} [(g(x_i) - g(x))^2] \quad (104)$$

$$\leq \frac{1}{m} \sum_{i \in [m]} \kappa^2 \rho^2 = \kappa^2 \rho^2. \quad (105)$$

Thus,  $f_{\text{eig}}$  satisfies Assumption 4.2 with  $\epsilon = \kappa^2 \rho^2$ .

Since the data in the same  $S_i$  have the same downstream label, we know that Assumption 4.3 holds with  $B = \sqrt{r}$  and  $\alpha = 0$ . Thus, applying Theorem 4.4 finishes the proof for the upper bound.

For the lower bound, Let set  $\tilde{S}$  be the union of the  $\frac{1}{2}r_0$  sets among those  $r_0$  clusters that have the largest sizes. When  $k \leq \frac{1}{2} \cdot r_0$ , we can construct a function that maps all data in  $\tilde{S}$  to 0, hence the final error would be at least  $\frac{1}{2}$ .  $\square$

### D.4 Proof for Example 5.10

*Proof of Theorem 5.12.* For any vector  $h \in \{-1, 1\}^s$ , we define function  $\text{bin}(h) \in \{0, 1, \dots, 2^s - 1\}$  be the function that maps  $h$  to the corresponding number when viewing  $\frac{1}{2}(h + 1)$  as binary. Since  $\text{bin}(\cdot)$  is a one-to-one mapping, we can define  $U \in \{k \times s\}$  such that the  $i$ -th row of  $U$  equal to  $\frac{\sqrt{k}}{\gamma-1} \cdot \text{bin}^{-1}(i-1)$ . Let bias vector  $b \in \mathbb{R}^k$  be such that every dimension is  $\frac{\sqrt{k}}{\gamma-1}(-s - (\gamma-1)(s-1))$ . We have  $f_{U,b}^{\text{conv}}(x) = \sqrt{k} \cdot e_{\text{bin}(x_{t:t+s-1})+1} \in \mathbb{R}^k$ , where  $t$  is the starting position of the informative patch in  $x$ .

It can be verified that  $\mathbb{E}_{x \sim p_{\text{data}}}[f_{U,b}^{\text{conv}}(x) f_{U,b}^{\text{conv}}(x)^\top] = \mathbb{I}$  and  $\mathbb{E}_{(x,x^+) \sim p_{\text{pos}}} \left[ \left\| f_{U,b}^{\text{conv}}(x) - f_{U,b}^{\text{conv}}(x^+) \right\|_2^2 \right] = 0$ . Also, Assumption 4.3 holds with  $B = 1$  when viewing  $f_{\text{eig}} = f_{U,b}^{\text{conv}}$ .

Suppose some function  $f_{\hat{U},\hat{b}}^{\text{conv}}$  and dimension  $i \in [k]$  satisfies

$$\mathbb{E}_{(x,x^+) \sim p_{\text{pos}}} \left[ \left( f_{\hat{U},\hat{b}}^{\text{conv}}(x)_i - f_{\hat{U},\hat{b}}^{\text{conv}}(x^+)_i \right)^2 \right] = 0. \quad (106)$$

Then, we know that for any  $x \in p_{\text{data}}$ , suppose we define  $\tilde{x}$  as the vector that replaces spurious dimensions of  $x$  with 0. Notice that  $\tilde{x}$  is in the support of  $x$ 's augmentations, and the model is continuous, we know  $f_{\hat{U},\hat{b}}^{\text{conv}}(x)_i = f_{\hat{U},\hat{b}}^{\text{conv}}(\tilde{x})_i$ . Further notice that for any two data  $x, x'$  with the same informative patch (location might be different) and corresponding  $\tilde{x}, \tilde{x}'$ , there must be  $f_{\hat{U},\hat{b}}^{\text{conv}}(\tilde{x})_i = f_{\hat{U},\hat{b}}^{\text{conv}}(\tilde{x}')_i$  due to the structure of the convolutional neural networks. Thus, We have  $f_{\hat{U},\hat{b}}^{\text{conv}}(x)_i =$

$f_{\hat{U}, \hat{b}}^{\text{conv}}(x')_i$ . This suggests that the function  $f_{\hat{U}, \hat{b}}^{\text{conv}}(\cdot)_i$  is in the span of  $f_{U, b}^{\text{conv}}$ , hence finishes the proof for the upper bound.

For the lower bound, we note that due to the lack of invariance to informative patch location, we can construct a network with  $d \cdot 2^s$ -dimensional output that satisfies equation 15 and equation 16. When the output dimension is less than  $d \cdot 2^{s-1}$ , there would exist a minimizer of the contrastive loss that merges  $d \cdot 2^{s-1}$  pairs of clusters. If every pair of clusters has different downstream labels, there would be at least  $\frac{1}{2}$  loss incurred due to the data being mapped to the same feature, hence finishes the proof for the lower bound.  $\square$